NASA TECHNICAL REPORT

NASA TR R-358

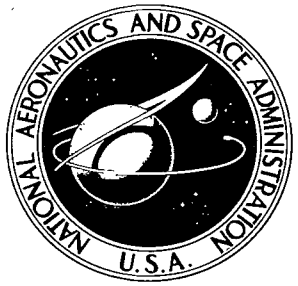

STRESS-INTENSITY FACTOR FOR A CRACKED SHEET WITH RIVETED AND UNIFORMLY SPACED STRINGERS

by C. C. Poe, Jr.

Langley Research Center
Hampton, Va. 23365

NATIONAL AERONAUTICS AND SPACE ADMINISTRATION • WASHINGTON, D. C. • MAY 1971

1. Report No.	2. Government Accession No.	3. Recipient's Catalog No.
NASA TR R-358		

4. Title and Subtitle	5. Report Date
STRESS-INTENSITY FACTOR FOR A CRACKED SHEET WITH RIVETED AND UNIFORMLY SPACED STRINGERS	6. Performing Organization Code: May 1971
7. Author(s): C. C. Poe, Jr.	8. Performing Organization Report No.: L-6826
9. Performing Organization Name and Address: NASA Langley Research Center, Hampton, Va. 23365	10. Work Unit No.: 126-14-15-01
	11. Contract or Grant No.
12. Sponsoring Agency Name and Address: National Aeronautics and Space Administration, Washington, D.C. 20546	13. Type of Report and Period Covered: Technical Report
	14. Sponsoring Agency Code

15. Supplementary Notes

16. Abstract

The stress-intensity factor and forces in the most highly loaded rivet and stringer were calculated for a cracked sheet with riveted and uniformly spaced stringers. Two symmetrical cases of crack location were considered – the case of a crack extending equally on both sides of a stringer and the case of a crack extending equally on both sides of a point midway between two stringers. The complete results are presented on design graphs for systematic variations of crack length, rivet spacing, stringer spacing, and stringer stiffness. The results show that the stress-intensity factor for the stiffened sheet is significantly less than that for an unstiffened sheet, except for crack lengths much less than the stringer spacing. Also, the forces in the most highly loaded stringer and rivet asymptotically approach limiting values for increasing crack length. The stress-intensity factor and the limiting values of the stringer and rivet forces are smaller for stiffer or more closely spaced stringers or for more closely spaced rivets.

17. Key Words (Suggested by Author(s))	18. Distribution Statement
Stress-intensity factor Crack Stiffened panel	Unclassified – Unlimited

19. Security Classif. (of this report)	20. Security Classif. (of this page)	21. No. of Pages	22. Price*
Unclassified	Unclassified	62	$3.00

*For sale by the National Technical Information Service, Springfield, Virginia 22151

STRESS-INTENSITY FACTOR FOR A CRACKED SHEET WITH RIVETED AND UNIFORMLY SPACED STRINGERS

By C. C. Poe, Jr.
Langley Research Center

SUMMARY

The stress-intensity factor and forces in the most highly loaded rivet and stringer were calculated for a cracked sheet with riveted and uniformly spaced stringers. Two symmetrical cases of crack location were considered – the case of a crack extending equally on both sides of a stringer and the case of a crack extending equally on both sides of a point midway between two stringers. The complete results are presented as design graphs for systematic variations of crack length, rivet spacing, stringer spacing, and stringer stiffness. The results show that the stress-intensity factor for the stiffened sheet is significantly less than that for an unstiffened sheet, except for crack lengths much less than the stringer spacing. Also, the forces in the most highly loaded stringer and rivet asymptotically approach limiting values for increasing crack length. The stress-intensity factor and the limiting values of the stringer and rivet forces are smaller for stiffer or more closely spaced stringers or for more closely spaced rivets.

INTRODUCTION

The design of a complex structure for maximum residual strength and maximum resistance to fatigue-crack propagation requires quantitative knowledge of the stresses in stiffened panels containing cracks. In recent years, considerable progress has been made in the stress analysis of cracked bodies by specifying a stress singularity near the crack tips. The stress-intensity factor, a parameter that describes the intensity of the singular stress field, has been used successfully to estimate fracture strength and fatigue-crack growth rates in situations where the assumptions of linear elasticity are valid. However, the stress-intensity factor (or some similar parameter) has been calculated only for simple configurations and panels with one or two stringers (refs. 1 to 10). Existing knowledge of stiffened panels is limited to experiments with box beams and tension panels (refs. 11 to 15).

In the present investigation, the stress-intensity factor and the forces in the most highly loaded rivet and stringer were calculated for a cracked sheet with riveted and uniformly spaced stringers. The unknown rivet forces were determined by requiring the

displacements at the rivets in the sheet and stringers to be equal. The stress-intensity factor for the cracked sheet was determined by superimposing the stress-intensity factors for the rivet forces and for the applied uniaxial stress. Two cases of symmetrical crack location were considered – the case of a crack extending equally on both sides of a stringer and the case of a crack extending equally on both sides of a point midway between two stringers. Although the points of attachment are referred to as being riveted, the results apply equally well to spotwelded attachments.

The salient effects of independently varying stringer stiffness, stringer spacing, rivet spacing, and crack length are discussed in detail. The complete results for systematic variations of stringer stiffness, stringer spacing, rivet spacing, and crack length are presented in the form of design graphs.

SYMBOLS

A_{ij}	displacement at ith rivet because of force of unity at jth rivet
a	half-crack length
B_i	displacement at ith rivet because of applied uniaxial stress of unity
b	stringer spacing
b_o	specific value of stringer spacing
d	rivet diameter
E	Young's modulus of elasticity
F	maximum force in stringer
K	stress-intensity factor
$\overline{K}$	stress-intensity-factor coefficient for rivet forces
L	stringer-load-concentration factor
P	point force applied to surface of crack

p	rivet spacing
Q	rivet force
r,θ	plane polar coordinates
S	applied uniaxial stress
t	thickness
v	y-component of displacement
w	stringer width
x,y	rectangular Cartesian coordinates
x_o,y_o	rivet coordinates
Z	Westergaard stress function
z	complex variable
α	stringer-spacing reduction parameter
$\alpha_1,\alpha_2,\alpha_3,\alpha_4$	functions defined on page 17
Γ	function defined on page 17
Λ	function defined on page 18
μ	ratio of stringer stiffness to total stiffness
ν	Poisson's ratio
ξ	distance from origin to point on crack surface
ρ_1,ρ_2	functions defined on page 14
σ_{xx},σ_{yy}	normal-stress components

$\bar{\sigma}_{yy}$ normal stress acting on crack surface

$\tau_{xy},\tau_{xz},\tau_{yz}$ shearing-stress components

ϕ_1,ϕ_2 functions defined on page 14

Ω function defined on page 16

Subscripts:

A pertaining to part A of sketch (g)

B pertaining to part B of sketch (g)

i at ith rivet

j at jth rivet

lim limiting

s stringer

Superscript:

s stringer

FORMULATION OF PROBLEM

Unknown Rivet Forces

Sketch (a) shows a sheet stiffened by stringers of uniform size and spacing. The stringers are attached to the sheet with equally spaced rivets, and the sheet and stringers are subjected to the uniaxial stresses S and $S\frac{E_s}{E}$, respectively, which produce equal longitudinal strains at large distances from the crack. The sheet contains a crack that is located symmetrically with respect to the stringers; that is, a crack that extends equally on both sides of a stringer or equally on both sides of a point midway between two stringers. The crack is assumed to be coincident with a row of rivets. (The results in ref. 9 indicate that this is the most critical case.)

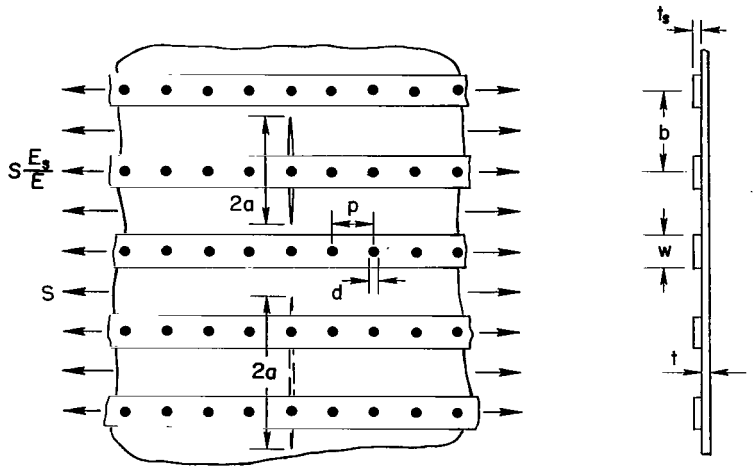

Sketch (a)

Sketch (b) shows the rivet forces acting symmetrically with respect to the crack when the crack extends equally on both sides of a stringer. The forces are also symmetrical for the other crack location. The row of rivets collinear with the crack exert no force because of symmetry. As required by equilibrium, the rivet forces act in opposite directions on the sheet and stringers. All forces acting on the sheet and stringers were assumed to act at the midplane of the sheet.

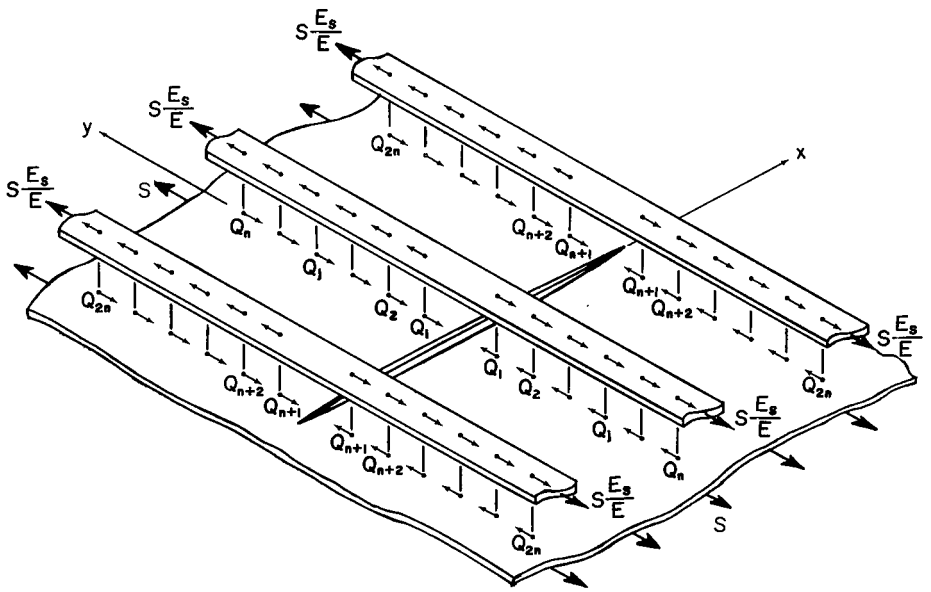

Sketch (b)

The equations necessary to determine the unknown rivet forces Q_j were obtained by equating the displacements at the rivet locations in the sheet and stringers. The displacements were written in terms of the following influence coefficients: A_{ij} and B_i, which represent the displacements in the cracked sheet at the ith rivet because of unit values of Q_j and S, respectively; and A_{ij}^S and B_i^S, which represent the displacements in the stringers at the ith rivet because of unit values of Q_j and $S\frac{E_S}{E}$, respectively. Thus, the displacement at the ith rivet in the sheet and stringers can be written

$$v_i = -\sum_j A_{ij}Q_j + B_iS \tag{1}$$

and

$$v_i^S = \sum_j A_{ij}^S Q_j + B_i^S \frac{E_S}{E} S \tag{2}$$

respectively, where i and j refer to only those rivets in one quadrant of the sheet. The negative sign was introduced in equation (1) because the rivet forces act in opposite directions on the sheet and stringers. Equating the displacements in equations (1) and (2) and collecting terms gives

$$\sum_j \left(A_{ij} + A_{ij}^S\right)Q_j - \left(B_i - \frac{E_S}{E} B_i^S\right)S = 0 \qquad (i = 1, 2, 3, \ldots) \tag{3}$$

A truncated set of these simultaneous equations was solved for the unknown rivet forces. The expressions for the influence coefficients in equations (3) are given in appendix A.

Stress-Intensity Factor for Stiffened Sheet

For the symmetrical case of plane extension (mode I), the stresses near the crack tip in sketch (c) can be written as (ref. 16)

$$\sigma_{xx} = \frac{K}{\sqrt{2\pi r}} \cos\frac{\theta}{2}\left(1 - \sin\frac{\theta}{2}\sin\frac{3\theta}{2}\right)$$

$$\sigma_{yy} = \frac{K}{\sqrt{2\pi r}} \cos\frac{\theta}{2}\left(1 + \sin\frac{\theta}{2}\sin\frac{3\theta}{2}\right)$$

$$\tau_{xy} = \frac{K}{\sqrt{2\pi r}} \sin\frac{\theta}{2}\cos\frac{\theta}{2}\cos\frac{3\theta}{2}$$

$$\tau_{xz} = \tau_{yz} = 0$$

where K is the stress-intensity factor, and terms containing higher powers of r have been neglected.

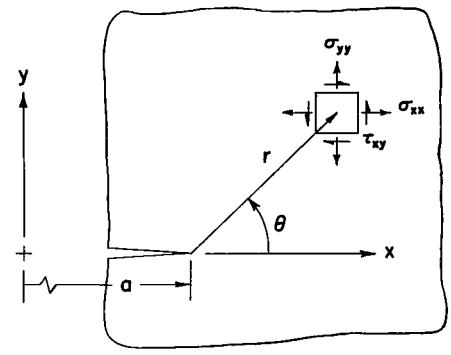

Sketch (c)

Because of symmetry, the uniaxial stress S and the symmetrical array of rivet forces produce only an opening mode of crack deformation in the stiffened sheet. By using the principle of superposition, the total-stress-intensity factor can be written as

$$K = S\sqrt{\pi a} + \sum_{j} \overline{K}_j Q_j \tag{4}$$

where $S\sqrt{\pi a}$ is the component due to the uniaxial stress S, and $\overline{K}_j Q_j$ is the component due to the symmetrical set of rivet forces Q_j. For the case of plane stress, the coefficient $\overline{K}$ is given (see ref. 17) for the symmetrical set of point forces shown in sketch (d) as

$$\overline{K} = \frac{\sqrt{\pi a}}{\pi t}\left[(3 + \nu)\Phi_1 - (1 + \nu)\Phi_2\right] \tag{5}$$

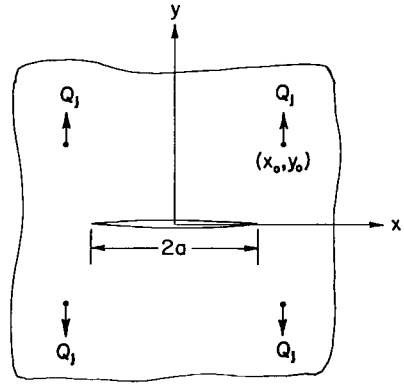

Sketch (d)

where

$$\Phi_1 = \frac{\gamma}{\sqrt{\left(x_o^2 - y_o^2 - a^2\right)^2 + 4x_o^2y_o^2}}$$

$$\Phi_2 = \frac{\left[\left(x_o^2 + a^2\right)y_o^2 + \left(x_o^2 - a^2\right)^2\right]\gamma^2 + x_o^2y_o^2\left(x_o^2 + y_o^2 - a^2\right)}{\gamma\left[\left(x_o^2 - y_o^2 - a^2\right)^2 + 4x_o^2y_o^2\right]^{3/2}}$$

and

$$\gamma = \frac{1}{\sqrt{2}}\left[\sqrt{\left(x_o^2 - y_o^2 - a^2\right)^2 + 4x_o^2y_o^2} - \left(x_o^2 - y_o^2 - a^2\right)\right]^{1/2}$$

(An error in ref. 17 has been corrected in Φ_2 of eq. (5).) In equations (4) and (5), the assumption is made that there are no rivet holes along the row of rivets through which the crack is assumed to advance. The results in reference 18 for a crack extending from or into a hole indicate that the effect of the holes on the stress-intensity factor is negligible except when the crack tip is within approximately a diameter of the hole. Thus, equations (4) and (5) will be accurate except when the crack tip is close to a rivet hole.

Stringer-Load-Concentration Factor

For convenience, a stringer-load-concentration factor L is defined as the ratio of the maximum force in the stringer to the remote force applied to the stringer

$$L = \frac{FE}{wt_sSE_s} \tag{6}$$

For a stringer that spans the crack, the rivet forces oppose the opening of the crack and, therefore, transfer load from the sheet to the stringer. Thus, the maximum force in a stringer occurs between the crack and the rivet on either side nearest the crack. The force at this location in the stringer is

$$F = \frac{wt_sSE_s}{E} + \sum_j Q_j \tag{7}$$

By substituting equation (7) into equation (6)

$$L = 1 + \frac{E}{wt_sSE_s}\sum_j Q_j \tag{8}$$

Numerical Solution

Because the stresses in the sheet at large distances from the crack are unaffected by the presence of the crack, the rivet forces are negligibly small except in the vicinity of the crack. In the present investigation only those rivets within the rectangular region shown in sketch (e) were included in the solution of equations (3). The height of the region

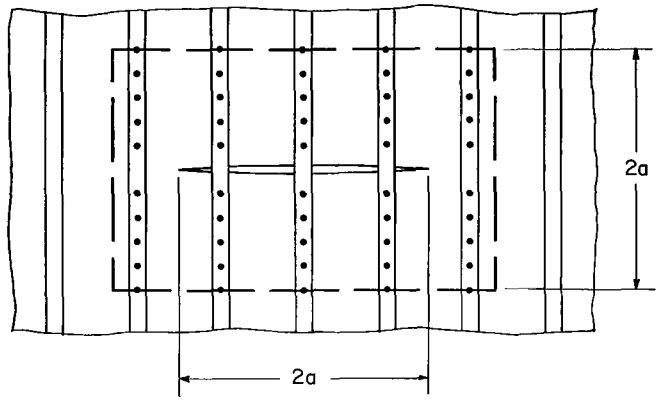

Sketch (e)

was chosen to be equal to the crack length $2a$ or to include 20 rivets per stringer, whichever was larger. The width of the region extended beyond the crack tips to include the next stringers. (Because of symmetry, only those rivet forces in one quadrant of this area were actually considered as unknowns in the solution of eqs. (3).) From preliminary calculations the computed value of the stress-intensity factor was found to be affected by less than 1 percent when the size of this region was increased.

RESULTS AND DISCUSSION

Preliminary calculations revealed that a variation in stringer width (for a given value of stringer stiffness) and a variation in rivet diameter had only a small effect on the results. This finding is consistent with that reported previously for a single stringer in reference 9. Thus, values of $d/p = 1/4$ and $w/d = 5$ were used to represent stringer width and rivet diameter. Also, a value of $\nu = 0.3$ was used for Poisson's ratio in both the sheet and stringers.

The parameters that were found to have a significant effect on the results are rivet spacing, stringer spacing, stringer stiffness, and crack length. The following subsections contain discussions of the salient effects of these parameters on the stress-intensity factor and the forces in the most highly loaded rivet and stringer.

Appendix B presents graphs of the stress-intensity factor and the forces in the most highly loaded rivet and stringer for systematic variations of the significant parameters. Thus, these graphs may be used as design graphs.

Stress-Intensity Factor

Figure 1 shows the effect of stringer stiffness on the relationship between the stress-intensity factor and half-crack length for a crack extending equally on both sides of a stringer and a crack extending equally on both sides of a point midway between two stringers. The stress-intensity factor and the half-crack length and rivet spacing are made nondimensional by dividing by the stress-intensity factor of an unstiffened sheet $S\sqrt{\pi a}$ and the stringer spacing b, respectively. The ratio of rivet to stringer spacing is fixed at $p/b = 1/6$. The stiffness of the stringers is expressed as μ, the ratio of total stringer stiffness to total panel stiffness. For stringers of uniform size and spacing

$$\mu = \frac{wt_s E_s}{wt_s E_s + btE} \tag{9}$$

The curves show that the stress-intensity factor of the stiffened sheet is essentially equal to that of an unstiffened sheet when the crack length is small compared to stringer spacing. Moreover, for a crack located midway between two stringers, $K \approx S\sqrt{\pi a}$ for crack lengths up to one-half the stringer spacing. Thus, in cases where the crack length is small compared to the stringer spacing, the stringers may give little improvement to the strength of the cracked sheet. For longer cracks, however, the stringers can reduce the stress-intensity factor considerably below that of an unstiffened sheet, especially when the crack tip is slightly beyond a stringer as evidenced by the minimum points in the curves. It should again be pointed out that the assumption is made that there are no rivet holes along the row of rivets through which the crack is assumed to advance. However, the effect on the stress-intensity factor of such rivet holes is negligible except when the crack tip is within approximately one diameter of a hole. The curves for the various values of μ show that the stress-intensity factor is lower for stiffer stringers. The value of $\mu = 1$ represents the limiting case when the stiffness of the stringers becomes very large compared to the stiffness of the sheet and, thus, gives a lower bound on the stress-intensity factor. It is important to note that significant reductions in the stress-intensity factor occur for moderately stiff stringers. In fact, 80 percent of the maximum possible reduction in the stress-intensity factor occurs when the stringers are as stiff as the sheet ($\mu = 0.5$).

Figure 2 shows the effect of rivet spacing on the relationship between the stress-intensity factor and half-crack length for both crack locations. The stiffness of the

stringers is fixed at $\mu = 0.5$. The curves for various ratios of rivet to stringer spacing show that the stress-intensity factor is also lower for more closely spaced rivets. However, when the crack tip is near a stringer, the curves continue to decrease with decreasing rivet spacing, and very small minimum values occur in the curves at each stringer. Thus, the effectiveness of the stringers in arresting a crack may increase significantly with decreasing rivet spacing. It is important to note, however, that integral stringers (a limiting case of riveted stringers with small rivet spacing) are not the most effective stringers for arresting or impeding cracks because the crack front also tends to progress through the stringers. As the rivet spacing decreases, the stress-intensity factor approaches the lower bound, which corresponds to the case of a continuously attached stringer (ref. 9). When the crack tip is between stringers, this lower bound is apparently reached with the small rivet spacings.

Figure 3 shows the effect of stringer spacing on the relationship between the stress-intensity factor and half-crack length for both crack locations. The stiffness of the stringers is fixed at $\mu = 0.5$. In order to show directly the effect of stringer spacing, the half-crack length and rivet spacing are normalized by dividing by a fixed value of stringer spacing b_o where $p/b_o = 1/6$. The curves for the smaller values of stringer spacing, $\alpha = 1/2$ and $1/4$, show that the stress-intensity factor is also lower for more closely spaced stringers except at the minimum points. These exceptions occur at the minimum points because the more widely spaced stringers have a larger individual stiffness and, thus, a larger local effect. The curve for $\alpha = 1/4$ appears to represent a lower bound on the stress-intensity factor for decreasing stringer spacing.

It is important to note in figures 1 to 3 that the curves for the stress-intensity factor as a function of crack length have lower bounds for increasing stringer stiffness and decreasing rivet spacing and stringer spacing. Thus, optimum values of these parameters may exist when other design considerations are taken into account.

Force in Most Highly Loaded Stringer

Figures 4 to 6 show the effects of stringer stiffness, rivet spacing, and stringer spacing on the relationship between the force in the most highly loaded stringer and half-crack length. The force in the stringer is shown as the stringer-load-concentration factor L. The most highly loaded stringers were always the middle stringer or the middle two stringers, depending on the crack location.

The curves show that L is essentially unity for small cracks and increases with increasing crack length. For very long cracks, the curves approach limits that are independent of crack location. For stringers of uniform size and spacing, these limiting values can be shown to be the reciprocal of the stringer stiffness ratio μ. Consider the case in which the crack has progressed entirely across the width of the sheet. The force

that must be transferred from the sheet to the stringers is btS per stringer. By adding this increment to the applied force the limiting force in a stringer becomes

$$F_{lim} = \frac{wt_s E_s S}{E} + btS \tag{10}$$

By substituting equation (10) into equation (6) the limiting value of L becomes

$$L_{lim} = 1 + \frac{btE}{wt_s E_s} \tag{11}$$

The right-hand side of equation (11) is the reciprocal of the stringer stiffness ratio μ. (See eq. (9).) Thus,

$$L_{lim} = \mu^{-1} \tag{12}$$

Values of L_{lim} calculated by equation (12) are shown in figures 4 to 6 as horizontal dashed lines. The curves in figure 4 show that for small values of μ the stress in the most highly loaded stringer can be much larger than the stress applied remotely to the stringers. Therefore, stringers with small stiffness are more likely to fail than stringers with large stiffness when the sheet is cracked.

Figures 5 and 6 show that for larger rivet spacing and for larger stringer spacing longer cracks are required for L to reach L_{lim}.

Force in Most Highly Loaded Rivet

Figures 7 to 9 show the effect of stringer stiffness, rivet spacing, and stringer spacing on the relationship between the force in the most highly loaded rivet and the half-crack length. The rivet force was normalized with respect to the force btS, which is the maximum force that can be transferred from the cracked sheet to a stringer. The most highly loaded rivets were always the rivets nearest the crack in the most highly loaded stringers.

The curves show that the force in the rivet increases with crack length and asymptotically approaches a limiting value that is independent of crack location. For smaller stringer stiffness, larger rivet spacing, or larger stringer spacing, longer cracks are required for the rivet force to reach its limiting value. For cracks of intermediate length, the curves cross one another and general conclusions cannot be made about the effect of stringer stiffness, rivet spacing, or stringer spacing.

The limiting values of rivet force observed in figures 7 to 9 cannot be derived like those for the stringer force given by equation (12). However, values of rivet force for very long cracks were estimated from graphs of rivet force plotted against the inverse of crack length. These estimated values of limiting rivet force are plotted in figure 10 against μ for the various values of α and p/b. The curves show that the limiting value of rivet force is smaller for stiffer or more closely spaced stringers or for more closely spaced rivets.

CONCLUDING REMARKS

The stress-intensity factor and forces in the most highly loaded stringer and rivet were calculated for a cracked sheet with riveted and uniformly spaced stringers. The calculations were made for two symmetrical cases of crack location – the case of a crack extending equally on both sides of a stringer and the case of a crack extending equally on both sides of a point midway between two stringers. The results are presented in the form of design graphs for a systematic variation of crack length, stringer stiffness, rivet spacing, and stringer spacing.

For small cracks the stress-intensity factor for a stiffened sheet is essentially equal to that of an unstiffened sheet. For longer cracks the stress-intensity factor is reduced significantly by the stringers. The stress-intensity factor is smaller for stiffer or more closely spaced stringers or for more closely spaced rivets. However, the stress-intensity factor has a lower bound with respect to each of these parameters, and an optimum value of each parameter may exist when other design considerations are taken into account.

The forces in the most highly loaded rivet and stringer approach limiting values with increasing crack length. As in the case of the stress-intensity factor, these limiting values of force are smaller for stiffer or more closely spaced stringers or for more closely spaced rivets.

Langley Research Center,
National Aeronautics and Space Administration,
Hampton, Va., February 24, 1971.

APPENDIX A

EQUATIONS FOR DETERMINING INFLUENCE COEFFICIENTS OF CRACKED SHEET AND STRINGERS

Cracked Sheet

Applied uniaxial stress.- For the infinite sheet containing a crack in sketch (f), the displacement in the y-direction for a state of plane stress can be developed from reference 19 as

$$v = \frac{S}{E}\left\{2\sqrt{\rho_1\rho_2}\sin\left(\frac{\phi_1 + \phi_2}{2}\right) - y - (1 + \nu)\frac{y}{\sqrt{\rho_1\rho_2}}\left[x\cos\left(\frac{\phi_1 + \phi_2}{2}\right) + y\sin\left(\frac{\phi_1 + \phi_2}{2}\right) - \sqrt{\rho_1\rho_2}\right]\right\} \tag{13}$$

where

$$\rho_1 = \sqrt{(x - a)^2 + y^2}$$

$$\rho_2 = \sqrt{(x + a)^2 + y^2}$$

$$\phi_1 = \tan^{-1}\left(\frac{y}{x - a}\right)$$

$$\phi_2 = \tan^{-1}\left(\frac{y}{x + a}\right)$$

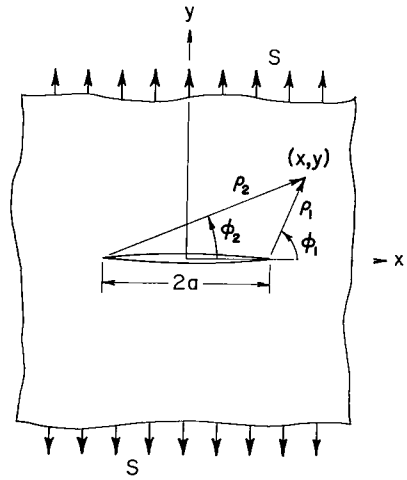

Sketch (f)

The influence coefficients B_i are determined from equation (13) by setting the stress S equal to unity.

Rivet forces.- The displacements for a cracked sheet with symmetrically applied point forces, shown as part C in sketch (g), are obtained by the addition of the displacements for parts A and B. Part A shows a sheet that is subjected to symmetrically applied point forces but does not contain a crack. The internal tensile stress σ_{yy} that exists along $y = 0$ between $|x| \leqq a$ is shown as $\bar{\sigma}_{yy}$. Part B shows a sheet that contains a crack along $y = 0$, $|x| \leqq a$, with the compressive stress $-\bar{\sigma}_{yy}$ applied to the crack surface. The addition of parts A and B therefore results in σ_{yy} being zero along $y = 0$, $|x| \leqq a$. The other boundary condition $\tau_{xy} = 0$ along $y = 0$ is satisfied by symmetry.

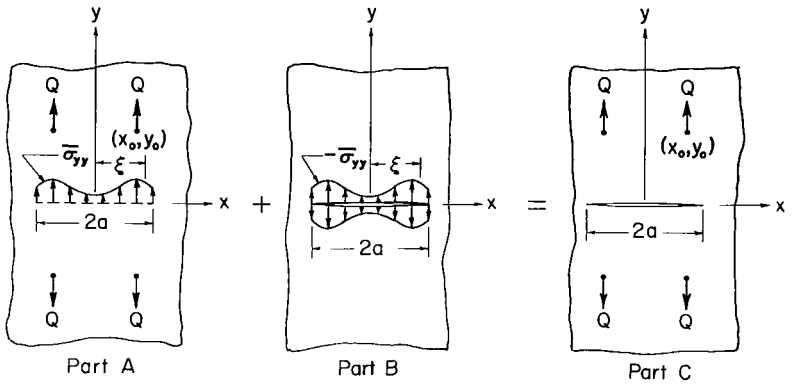

Sketch (g)

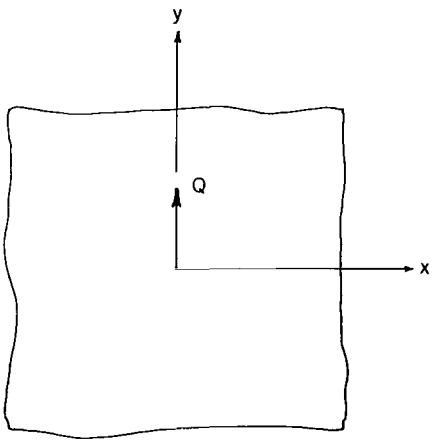

Sketch (h)

The stresses and displacements for part A of sketch (g) are determined from the solution for a single point force using superposition. The y-component of the stresses and displacements for the single point force shown in sketch (h) can be obtained from reference 20 for plane stress as

$$v = -\frac{(1+\nu)Q}{4\pi tE}\left[\frac{1}{2}(3-\nu)\ln(x^2+y^2) + (1+\nu)\left(\frac{x^2}{x^2+y^2}\right)\right] \tag{14}$$

and

$$\sigma_{yy} = -\frac{(1+\nu)Q}{4\pi t}\left(\frac{y}{x^2+y^2}\right)\left(\frac{3+\nu}{1+\nu} - \frac{2x^2}{x^2+y^2}\right) \tag{15}$$

Equation (14) cannot be used in its present form to calculate the displacement caused by the force Q because there is a singularity at the origin. To circumvent this problem, the point force Q is assumed to be distributed uniformly over the rivet diameter d. Replacing x by $x - \bar{x}$ in equation (14) and integrating with respect to $\bar{x}$ from $-\frac{1}{2}d$ to $\frac{1}{2}d$, the displacement becomes

$$v = -\frac{(1+\nu)(3-\nu)Q}{16\pi tE}\left\{\left(\frac{2x}{d}+1\right)\ln\left[\left(\frac{2x}{d}+1\right)^2 + \frac{4y^2}{d^2}\right]\right.$$

$$\left. - \left(\frac{2x}{d}-1\right)\ln\left[\left(\frac{2x}{d}-1\right)^2 + \frac{4y^2}{d^2}\right] + \left(\frac{1-\nu}{3-\nu}\right)\left(\frac{8y}{d}\right)\tan^{-1}\left(\frac{\frac{y}{d}}{\frac{x^2}{d^2}+\frac{y^2}{d^2}-\frac{1}{4}}\right)\right\} \tag{16}$$

For $d \to 0$, equation (16) reduces to equation (14). By translating the origin in equation (16) so that the point force is located at a point (x_o, y_o) and by adding the displacements for point forces located at $(\pm x_o, \pm y_o)$, the displacement field for part A of sketch (g) is written as

$$v_A = \frac{(1+\nu)(3-\nu)Q}{16\pi tE}\Omega \tag{17}$$

where

$$\Omega = (\alpha_1+1)\ln\left[\frac{(\alpha_1+1)^2+\alpha_4^2}{(\alpha_1+1)^2+\alpha_3^2}\right] - (\alpha_1-1)\ln\left[\frac{(\alpha_1-1)^2+\alpha_4^2}{(\alpha_1-1)^2+\alpha_3^2}\right]$$

$$+ (\alpha_2+1)\ln\left[\frac{(\alpha_2+1)^2+\alpha_4^2}{(\alpha_2+1)^2+\alpha_3^2}\right] - (\alpha_2-1)\ln\left[\frac{(\alpha_2-1)^2+\alpha_4^2}{(\alpha_2-1)^2+\alpha_3^2}\right]$$

$$+ 4\left(\frac{1-\nu}{3-\nu}\right)\left\{\alpha_4\left[\tan^{-1}\left(\frac{2\alpha_4}{\alpha_1^2+\alpha_4^2-1}\right) + \tan^{-1}\left(\frac{2\alpha_4}{\alpha_2^2+\alpha_4^2-1}\right)\right]\right.$$

$$\left. - \alpha_3\left[\tan^{-1}\left(\frac{2\alpha_3}{\alpha_1^2+\alpha_3^2-1}\right) + \tan^{-1}\left(\frac{2\alpha_3}{\alpha_2^2+\alpha_3^2-1}\right)\right]\right\}$$

and

$$\alpha_1 = \frac{2(x - x_o)}{d}$$

$$\alpha_2 = \frac{2(x + x_o)}{d}$$

$$\alpha_3 = \frac{2(y - y_o)}{d}$$

$$\alpha_4 = \frac{2(y + y_o)}{d}$$

By using the same procedure and equation (15), the stress field for part A of sketch (g) is written as

$$\sigma_{yy} = \frac{(1+\nu)Q}{\pi td}\left\{\frac{1}{2}\left(\frac{1-\nu}{1+\nu}\right)\left(\frac{\alpha_4}{\alpha_1^2+\alpha_4^2} + \frac{\alpha_4}{\alpha_2^2+\alpha_4^2} - \frac{\alpha_3}{\alpha_1^2+\alpha_3^2} - \frac{\alpha_3}{\alpha_2^2+\alpha_3^2}\right)\right.$$

$$\left. + \alpha_4\left[\left(\frac{\alpha_4}{\alpha_1^2+\alpha_4^2}\right)^2 + \left(\frac{\alpha_4}{\alpha_2^2+\alpha_4^2}\right)^2\right] - \alpha_3\left[\left(\frac{\alpha_3}{\alpha_1^2+\alpha_3^2}\right)^2 + \left(\frac{\alpha_3}{\alpha_2^2+\alpha_3^2}\right)^2\right]\right\} \qquad (18)$$

The stress $\bar{\sigma}_{yy}$ that must be removed in part A of sketch (g) is obtained from equation (18) by setting $y = 0$ and $x = \xi$. Thus,

$$\bar{\sigma}_{yy} = \frac{(1+\nu)Qy_o}{2\pi t}\Gamma \qquad (19)$$

where

$$\Gamma = \left(\frac{1-\nu}{1+\nu}\right)\left[\frac{1}{(\xi - x_o)^2 + y_o^2} + \frac{1}{(\xi + x_o)^2 + y_o^2}\right]$$

$$+ 2y_o\left\{\left[\frac{1}{(\xi - x_o)^2 + y_o^2}\right]^2 + \left[\frac{1}{(\xi + x_o)^2 + y_o^2}\right]^2\right\}$$

The displacement for part B of sketch (g) is determined by using the displacements for the point forces applied to the crack surface in sketch (i) as a pseudo-Green's function.

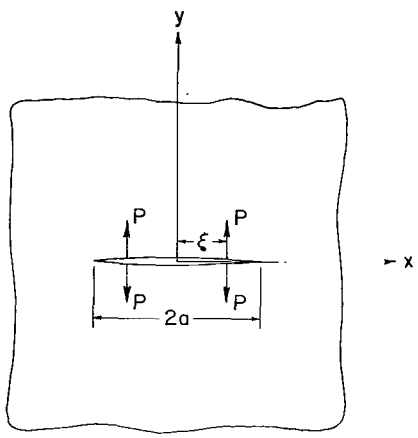

Sketch (i)

The Westergaard stress function (see ref. 21) for this problem is given as

$$Z = \frac{2Pz}{\pi t\left(z^2 - \xi^2\right)}\sqrt{\frac{a^2 - \xi^2}{z^2 - a^2}} \tag{20}$$

where z is the complex variable $x + iy$. For plane stress, the y-component of displacement is given by

$$v = \frac{1}{E}\left[2\,\mathrm{Im}(\overline{Z}) - (1 + \nu)y\mathrm{Re}(Z)\right] \tag{21}$$

where $\overline{Z}$ is the first integral of Z. By evaluating $\mathrm{Im}(\overline{Z})$ and $\mathrm{Re}(Z)$ from equation (20) and by substituting these into equation (21), the displacement is

$$v = \frac{P}{\pi tE}\Lambda \tag{22}$$

where

$$\Lambda = \ln\left(\frac{a^2 - \xi^2 + 2\sqrt{a^2 - \xi^2}\sqrt{C_1 + C_2} + 2C_2}{a^2 - \xi^2 - 2\sqrt{a^2 - \xi^2}\sqrt{C_1 + C_2} + 2C_2}\right)$$

$$- \frac{(1 + \nu)y\sqrt{a^2 - \xi^2}}{C_2}\left[\frac{x\left(x^2 + y^2 - \xi^2\right)\sqrt{C_2 - C_1} - y\left(x^2 + y^2 + \xi^2\right)\sqrt{C_1 + C_2}}{\left(x^2 - y^2 - \xi^2\right)^2 + 4x^2y^2}\right]$$

and

$$C_1 = \frac{1}{2}(a^2 + y^2 - x^2)$$

$$C_2 = \sqrt{C_1^2 + x^2y^2}$$

By substituting $t\bar{\sigma}_{yy}\,d\xi$ for P in equation (22) and by integrating with respect to ξ over the crack, the displacements for part B of sketch (g) become

$$v_B = \frac{1}{\pi E}\int_0^a \bar{\sigma}_{yy}\Lambda\,d\xi \tag{23}$$

Now, by substituting equation (19) for $\bar{\sigma}_{yy}$, equation (23) can be written

$$v_B = \frac{(1 + \nu)Qy_o}{2\pi^2 tE}\int_0^a \Lambda\Gamma\,d\xi \tag{24}$$

By adding the displacements for parts A and B (sketch (g)), which are given by equations (17) and (24), the displacement for a cracked sheet with symmetrically applied point forces becomes

$$v = \frac{(1 + \nu)Q}{16\pi tE}\left[(3 - \nu)\Omega + \frac{8y_o}{\pi}\int_0^a \Lambda\Gamma\,d\xi\right] \tag{25}$$

The integral in equation (25) is readily evaluated numerically on a digital computer.

The influence coefficients A_{ij} are determined from equation (25) by setting Q equal to unity.

Stringer

Applied uniaxial stress.- The y-component of displacement for the stringer in sketch (j) with the uniaxial stress SE_s/E is given simply by

$$v = \frac{Sy}{E} \tag{26}$$

The influence coefficients B_i^s are determined from equation (26) by setting SE_s/E equal to unity.

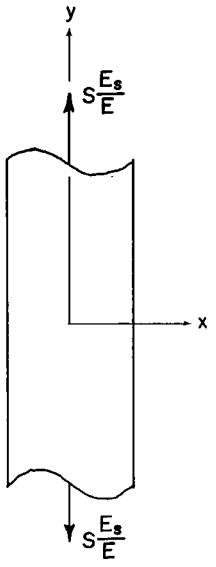

Sketch (j)

Rivet forces.- The displacements in the finite width stringer subjected to a pair of point forces in sketch (k) can be approximated by the displacements in the infinite sheet subjected to pairs of equal and uniformly spaced point forces. The only boundary condition for the finite width stringer that will not be satisfied is $\sigma_{xx} = 0$ along $x = \pm w/2$.

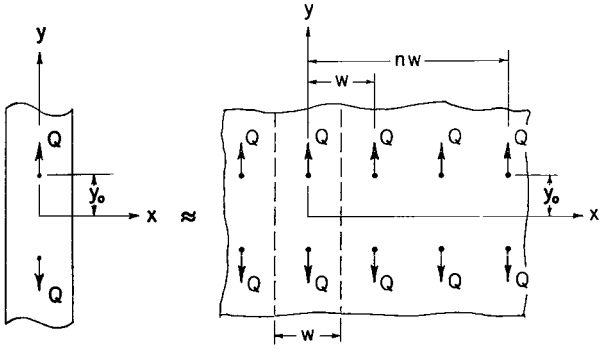

Sketch (k)

The y-component of displacement at a point (0,y) in the infinite sheet in sketch (k) is obtained by adding the displacements due to symmetrical sets of forces located at $(\pm nw, \pm y_o)$ given by equation (17). Thus

$$v = \frac{(1 + \nu)(3 - \nu)Q}{8\pi t_s E_s} \sum_{n=0}^{\infty} \psi_n \tag{27}$$

where

$$\psi_o = \ln\left(\frac{1 + \alpha_4^2}{1 + \alpha_3^2}\right) + 2\left(\frac{1 - \nu}{3 - \nu}\right)\left[\alpha_4 \tan^{-1}\left(\frac{2\alpha_4}{\alpha_4^2 - 1}\right) - \alpha_3 \tan^{-1}\left(\frac{2\alpha_3}{\alpha_3^2 - 1}\right)\right]$$

and

$$\psi_n = \left(1 - \frac{2nw}{d}\right) \ln\left[\frac{\left(1 - \frac{2nw}{d}\right)^2 + \alpha_4^2}{\left(1 - \frac{2nw}{d}\right)^2 + \alpha_3^2}\right] + \left(1 + \frac{2nw}{d}\right) \ln\left[\frac{\left(1 + \frac{2nw}{d}\right)^2 + \alpha_4^2}{\left(1 + \frac{2nw}{d}\right)^2 + \alpha_3^2}\right]$$

$$+ \left(\frac{1 - \nu}{3 - \nu}\right)\left\{\alpha_4 \tan^{-1}\left[\frac{2\alpha_4}{\left(\frac{2nw}{d}\right)^2 + \alpha_4^2 - 1}\right] - \alpha_3 \tan^{-1}\left[\frac{2\alpha_3}{\left(\frac{2nw}{d}\right)^2 + \alpha_3^2 - 1}\right]\right\}$$

for $n = 1, 2, \ldots$. The influence coefficients A_{ij}^s are determined from equation (27) by setting the rivet force Q equal to unity.

APPENDIX B

DESIGN GRAPHS

Figures 11 to 16 show graphs of the stress-intensity factor, the stringer-load-concentration factor for the most highly loaded stringer, and the rivet force for the most highly loaded rivet plotted against the ratio a/b for various values of the ratios p/b and μ. The stress-intensity factor and the rivet force are made nondimensional by dividing by the stress-intensity factor of an unstiffened sheet $S\sqrt{\pi a}$ and the force btS, respectively. Values of $d/p = 1/4$, $w/d = 5$, and $\nu = 0.3$ were used to represent the rivet diameter, stringer width, and Poisson's ratio, respectively. Although the points of attachment are referred to as being riveted, the results apply equally well to spot-welded attachments. The range in values of μ and the ratio p/b are sufficient to include most stiffener-sheet configurations. The curves are shown for values of $a/b \leq 3$ and, thus, include crack lengths up to six times the stringer spacing. The graphs are shown for two symmetrical cases of crack location – the case of a crack extending equally on both sides of a stringer and the case of a crack extending equally on both sides of a point midway between two stringers.

The curves for the symmetrical cases of crack location may be used to obtain an upper bound on the stress-intensity factor for a nonsymmetrical crack by entering a curve with the larger value of half-crack length. The row of rivet holes through which the crack is assumed to advance is not accounted for in the calculations for the stress-intensity factor. However, crack-propagation times calculated by using these values should be conservative because of the time required for a crack to initiate from a hole. The present stress-intensity-factor calculations are based on the classical linear theory of elasticity. Hence, caution should be exercised when applying the results to cases in which the stringers yield.

REFERENCES

1. Romualdi, J. P.; Frasier, J. T.; and Irvin, G. R.: Crack-Extension-Force Near a Riveted Stiffener. NRL Rep. 4956, U.S. Navy, Oct. 11, 1957.

2. Sanders, J. Lyell, Jr.: Effect of a Stringer on the Stress Concentration Due to a Crack in a Thin Sheet. NASA TR R-13, 1959. (Supersedes NACA TN 4207.)

3. Romualdi, James P.; and Sanders, Paul H.: Fracture Arrest by Riveted Stiffeners. AFOSR TR 60-174, U.S. Air Force, Oct. 1960.

4. Isida, Makoto; and Itagaki, Yoshio: Stress Concentration at the Tip of a Central Transverse Crack in a Stiffened Plate Subjected to Tension. Proceedings of the Fourth U.S. National Congress of Applied Mechanics, Vol. Two, Amer. Soc. Mech. Eng., c.1962, pp. 955-969.

5. Leybold, Herbert A.: A Method for Predicting the Static Strength of a Stiffened Sheet Containing a Sharp Central Notch. NASA TN D-1943, 1963.

6. Greif, Robert; and Sanders, J. L., Jr.: The Effect of a Stringer on the Stress in a Cracked Sheet. Trans. ASME, Ser. E: J. Appl. Mech., vol. 32, no. 1, Mar. 1965, pp. 59-66.

7. Isida, M.: The Effect of a Stringer on the Stress Intensity Factors for the Tension of a Cracked Wide Plate. Dept. Mech., Lehigh Univ., Sept. 1965.

8. Isida, M.; Itagaki, Y.; and Iida, S.: On the Crack Tip Stress Intensity Factor for the Tension of a Centrally Cracked Strip With Reinforced Edges. Dept. Mech., Lehigh Univ., Sept. 1965.

9. Bloom, J. M.; and Sanders, J. L., Jr.: The Effect of a Riveted Stringer on the Stress in a Cracked Sheet. Trans. ASME, Ser. E: J. Appl. Mech., vol. 33, no. 3, Sept. 1966, pp. 561-570.

10. Figge, I. E.; and Newman, J. C., Jr.: Prediction of Fatigue-Crack-Propagation Behavior in Panels With Simulated Rivet Forces. NASA TN D-4702, 1968.

11. Hardrath, Herbert F.; Leybold, Herbert A.; Landers, Charles B.; and Hauschild, Louis W.: Fatigue-Crack Propagation in Aluminum-Alloy Box Beams. NACA TN 3856, 1956.

12. Hardrath, Herbert F.; and Whaley, Richard E.: Fatigue-Crack Propagation and Residual Static Strength of Built-Up Structures. NACA TN 4012, 1957.

13. Hardrath, Herbert F.; and Leybold, Herbert A.: Further Investigation of Fatigue-Crack Propagation in Aluminum-Alloy Box Beams. NACA TN 4246, 1958.

14. Whaley, Richard E.; and Kurzhals, Peter R.: Fatigue-Crack Propagation in Aluminum-Alloy Tension Panels. NASA TN D-543, 1960.

15. Leybold, Herbert A.: Residual Static Strength of Aluminum-Alloy Box Beams Containing Fatigue Cracks in the Tension Covers. NASA TN D-796, 1961.

16. Paris, Paul C.; and Sih, George C.: Stress Analysis of Cracks. Fracture Toughness Testing and Its Applications. Spec. Tech. Publ. No. 381, Amer. Soc. Testing Mater., c.1965, pp. 30-81.

17. Paris, Paul C.: Application of Muskehlishvili's Methods to the Analysis of Crack Tip Stress Intensity Factors for Plane Problems. Pt. III. Inst. Research, Lehigh Univ., June 1960.

18. Newman, J. C., Jr.: Stress Analysis of Simply and Multiply Connected Regions Containing Cracks by the Method of Boundary Collocation. M.S. Thesis, Virginia Polytech. Inst., May 1969.

19. Westergaard, H. M.: Bearing Pressures and Cracks. J. Appl. Mech., vol. 6, no. 2, June 1939, pp. A-49 – A-53.

20. Love, A. E. H.: A Treatise on the Mathematical Theory of Elasticity. Fourth ed. (First Amer. Printing), Dover Publ., 1944, p. 209.

21. Irwin, G. R.: Analysis of Stresses and Strains Near the End of a Crack Traversing a Plate. Trans. ASME, Ser. E: J. Appl. Mech., vol. 24, no. 3, Sept. 1957, pp. 361-364.

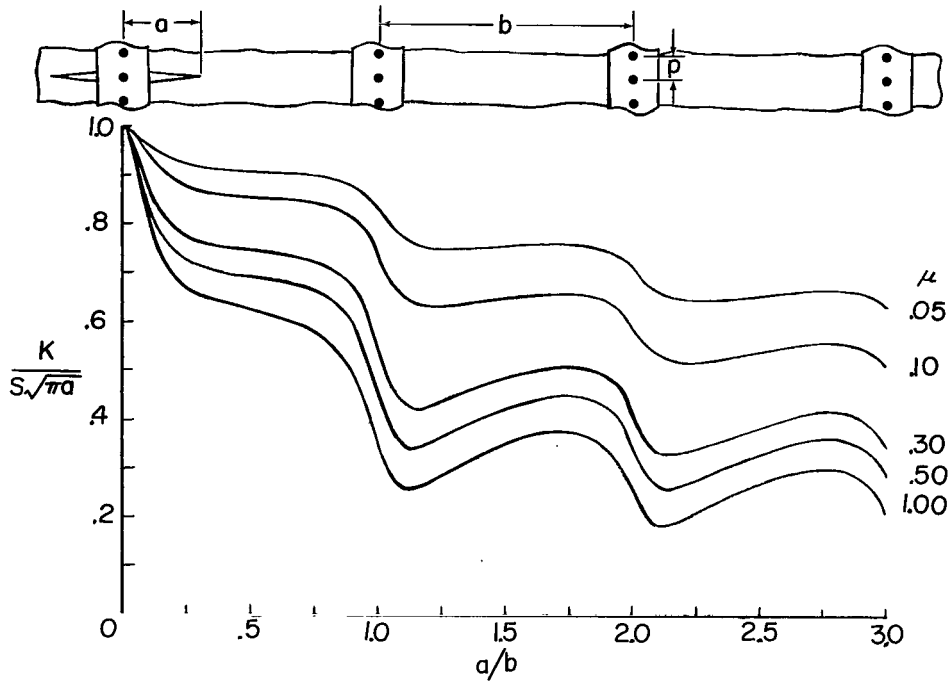

(a) Crack extending equally on both sides of stringer.

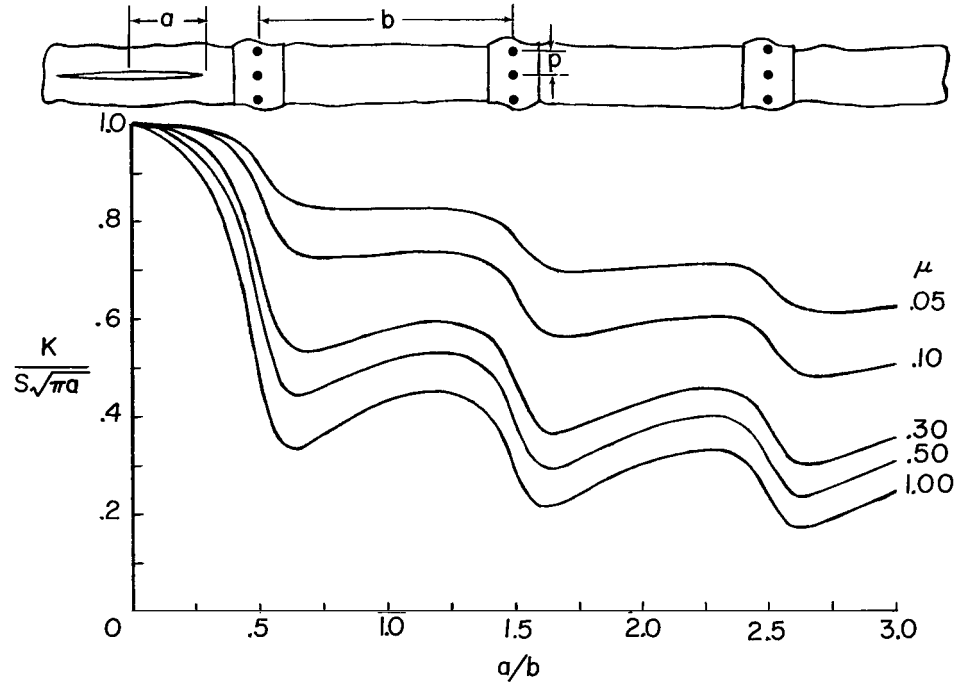

(b) Crack extending equally on both sides of point midway between two stringers.

Figure 1.- Effect of stringer stiffness on relationship between stress-intensity factor and crack length (p/b = 1/6).

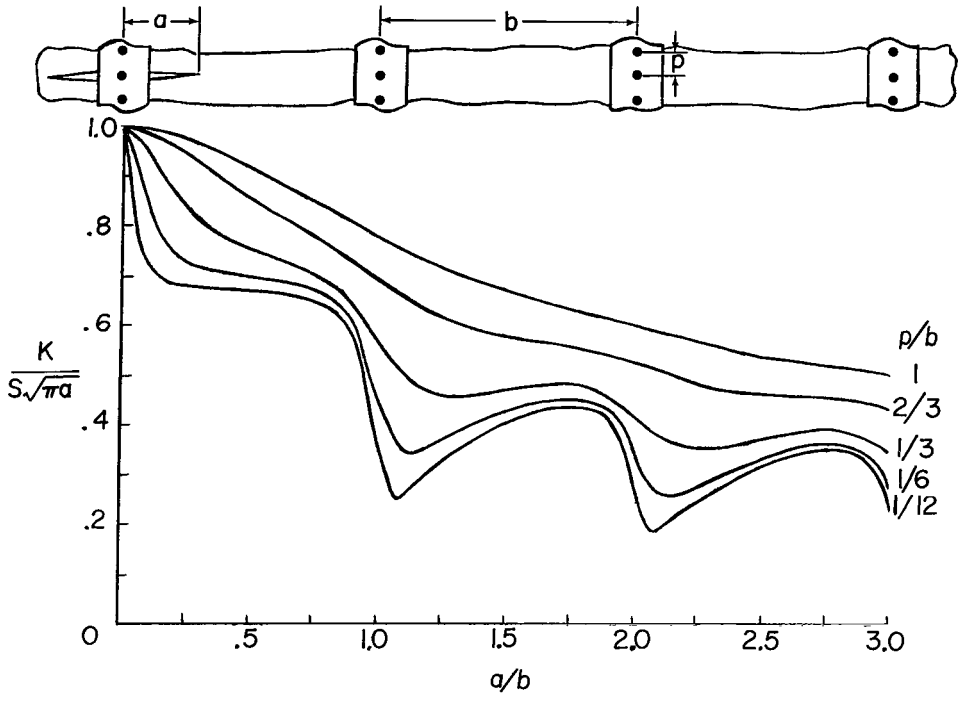

(a) Crack extending equally on both sides of stringer.

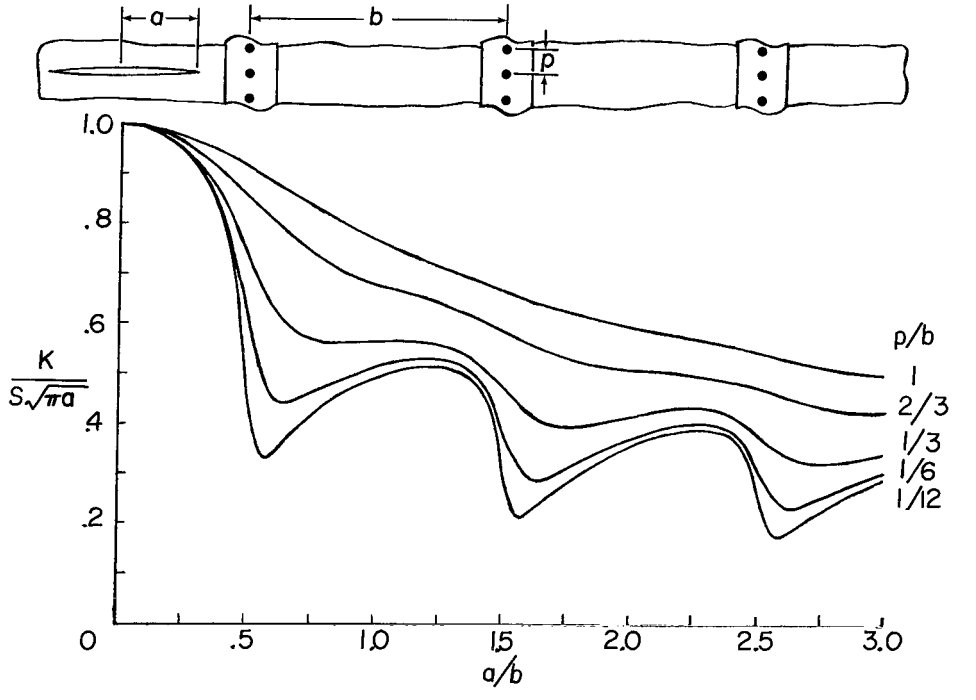

(b) Crack extending equally on both sides of point midway between two stringers.

Figure 2.- Effect of rivet spacing on relationship between stress-intensity factor and crack length ($\mu = 0.5$).

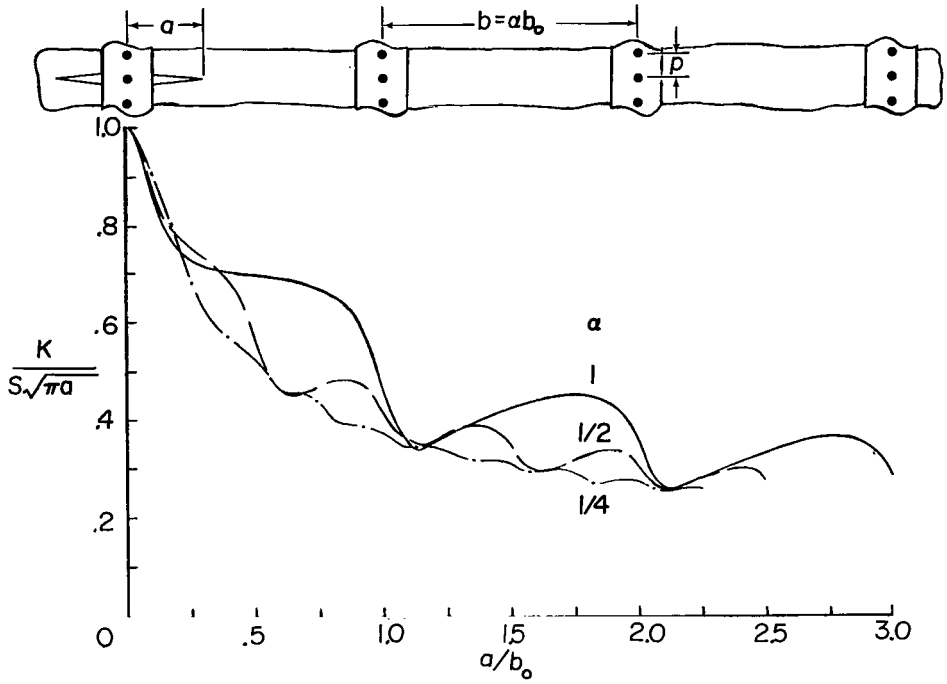

(a) Crack extending equally on both sides of stringer.

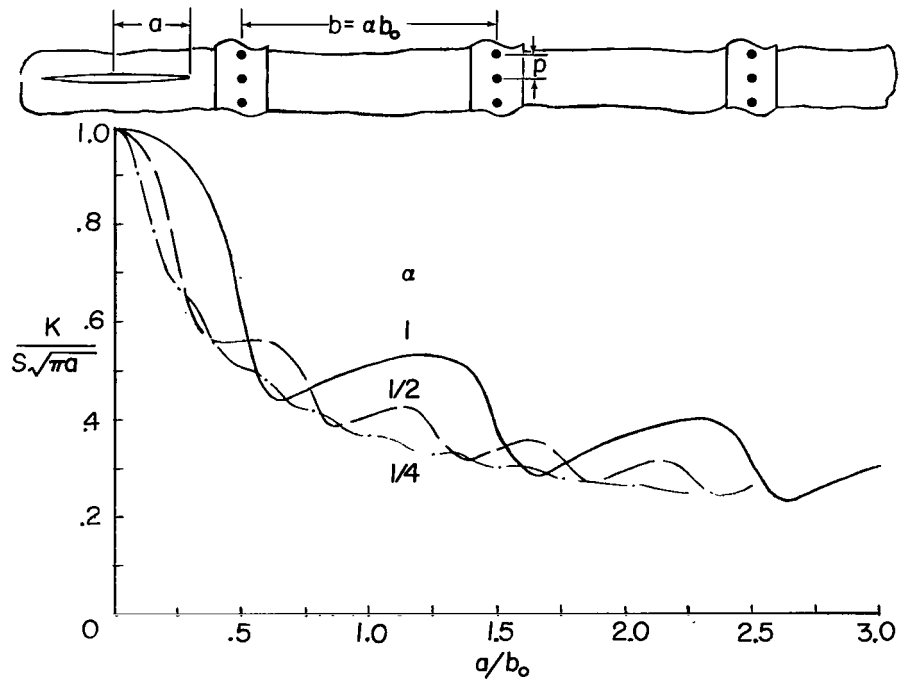

(b) Crack extending equally on both sides of point midway between two stringers.

Figure 3.- Effect of stringer spacing on relationship between stress-intensity factor and crack length $\left(p/b_o = 1/6 \text{ and } \mu = 0.5\right)$.

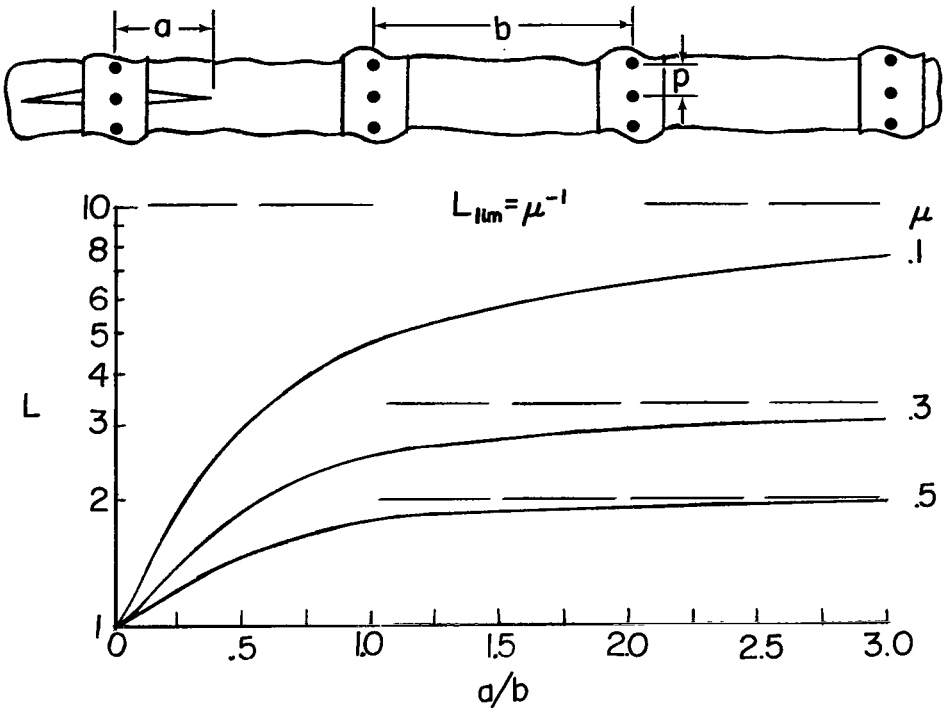

(a) Crack extending equally on both sides of stringer.

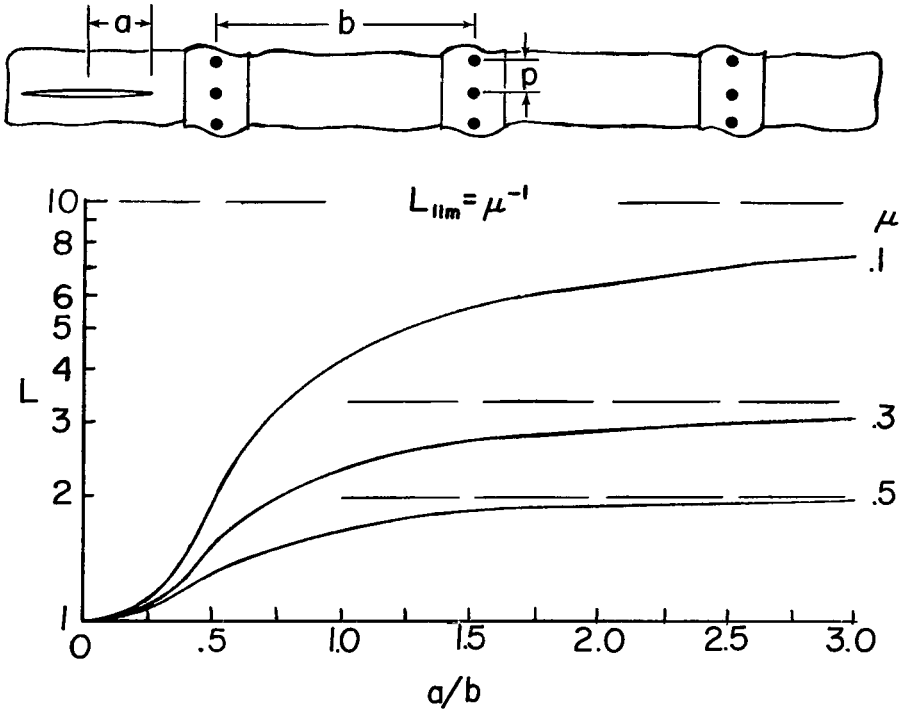

(b) Crack extending equally on both sides of point midway between two stringers.

Figure 4.- Effect of stringer stiffness on relationship between stringer-load-concentration factor and crack length for most highly loaded stringer (p/b = 1/6).

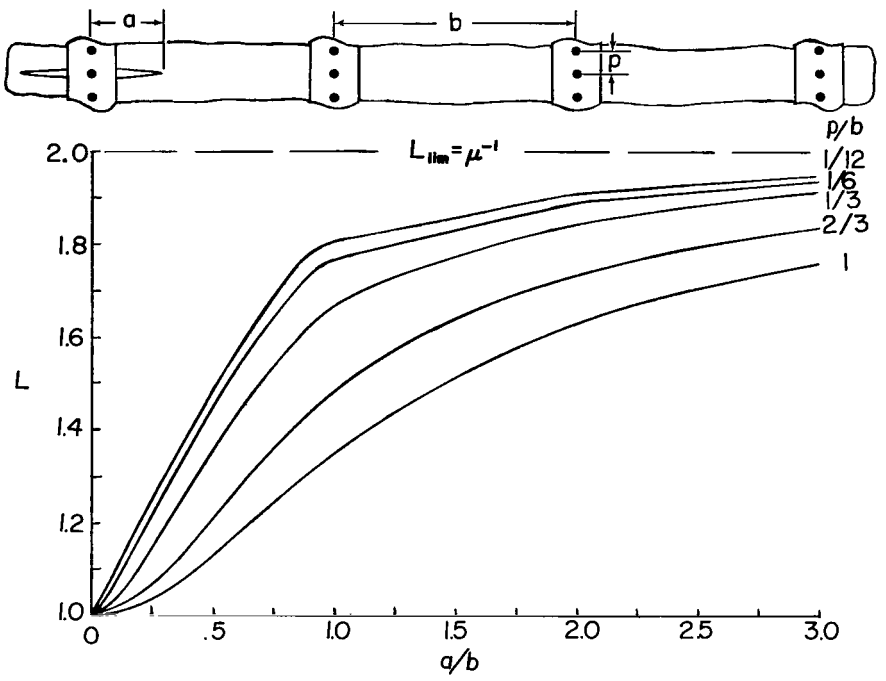

(a) Crack extending equally on both sides of stringer.

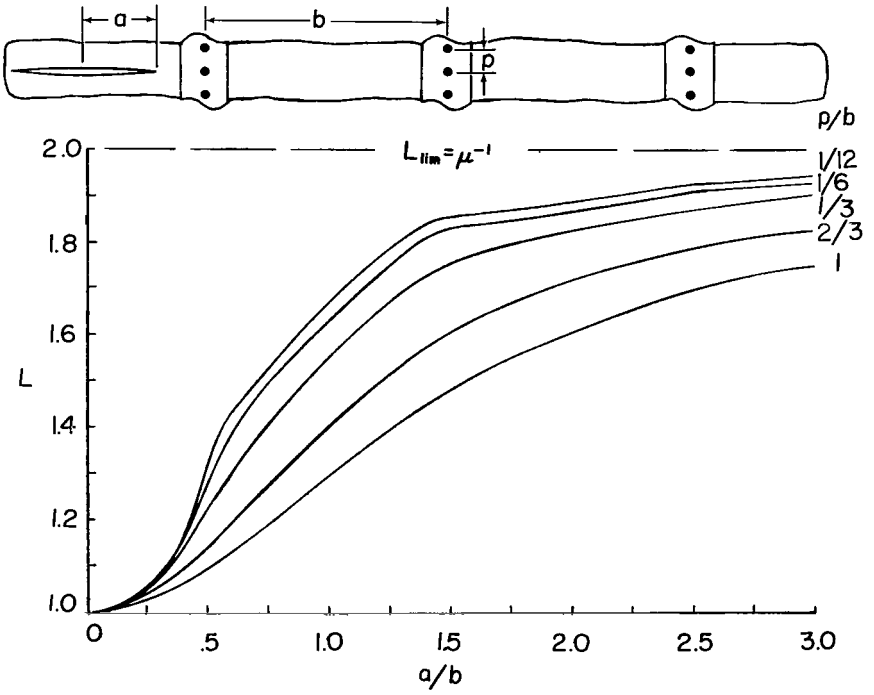

(b) Crack extending equally on both sides of point midway between two stringers.

Figure 5.- Effect of rivet spacing on relationship between stringer-load-concentration factor and crack length for most highly loaded stringer (μ = 0.5).

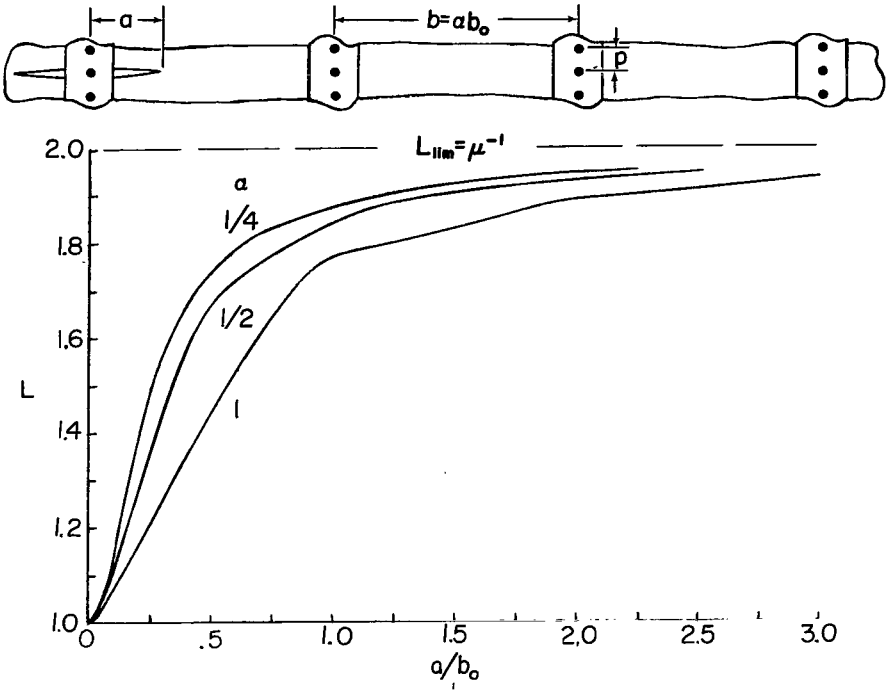

(a) Crack extending equally on both sides of stringer.

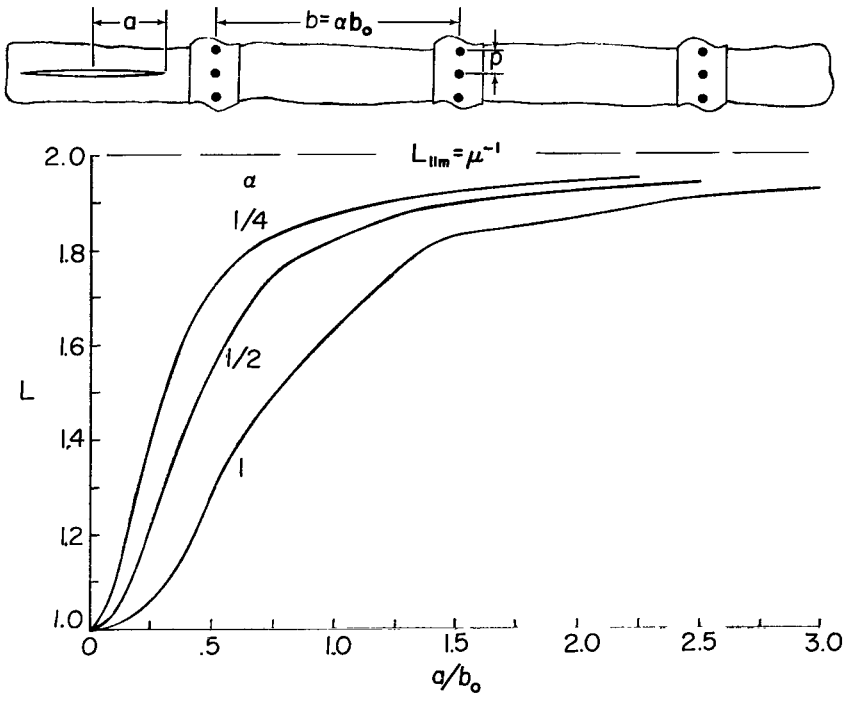

(b) Crack extending equally on both sides of point midway between two stringers.

Figure 6.- Effect of stringer spacing on relationship between stringer-load-concentration factor and crack length for most highly loaded stringer $\left(p/b_o = 1/6 \text{ and } \mu = 0.5\right)$.

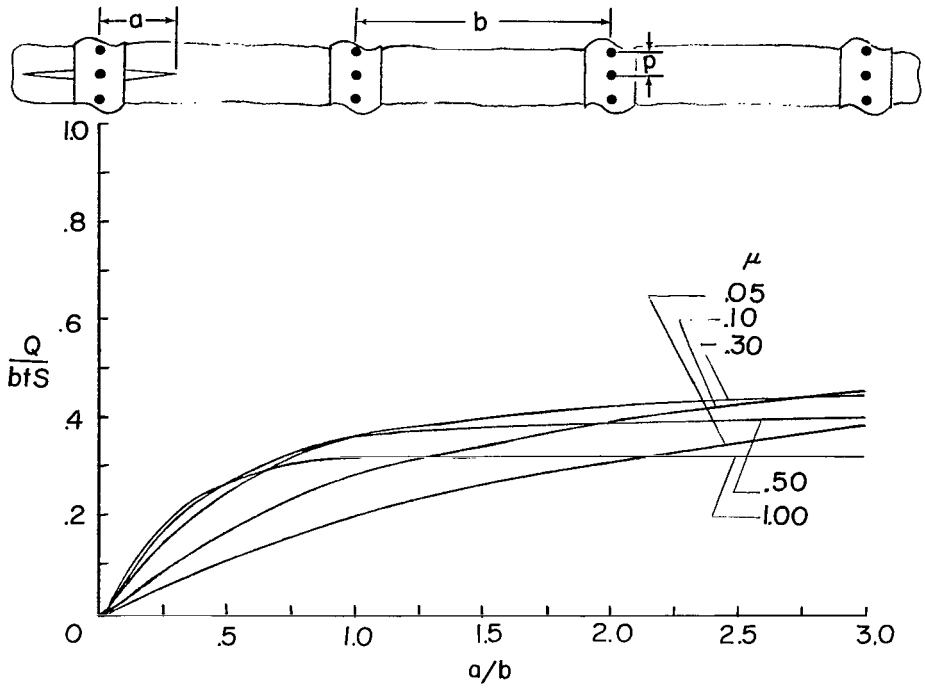

(a) Crack extending equally on both sides of stringer.

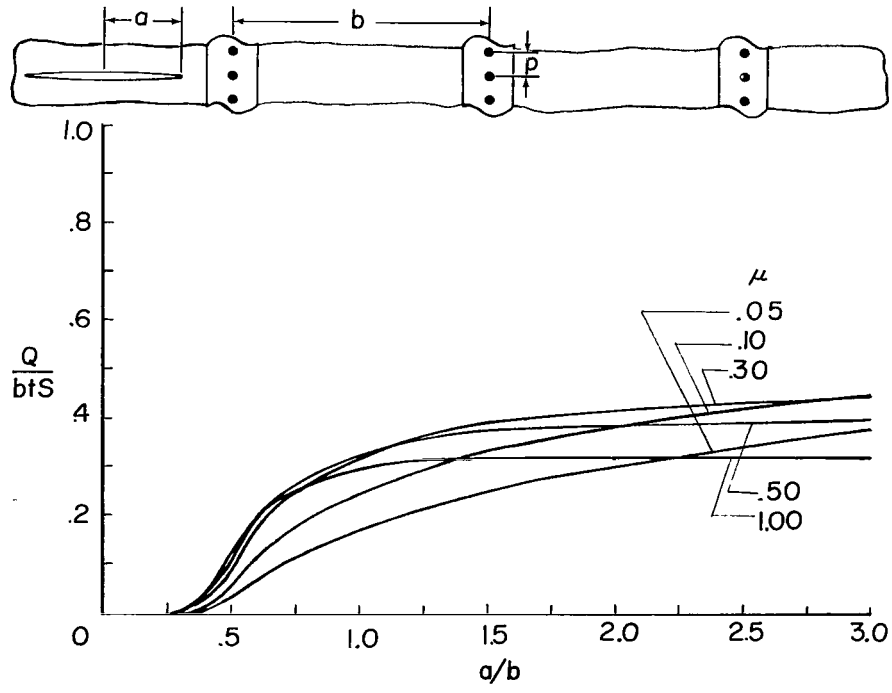

(b) Crack extending equally on both sides of point midway between two stringers.

Figure 7.- Effect of stringer stiffness on relationship between rivet force and crack length for most highly loaded rivet (p/b = 1/6).

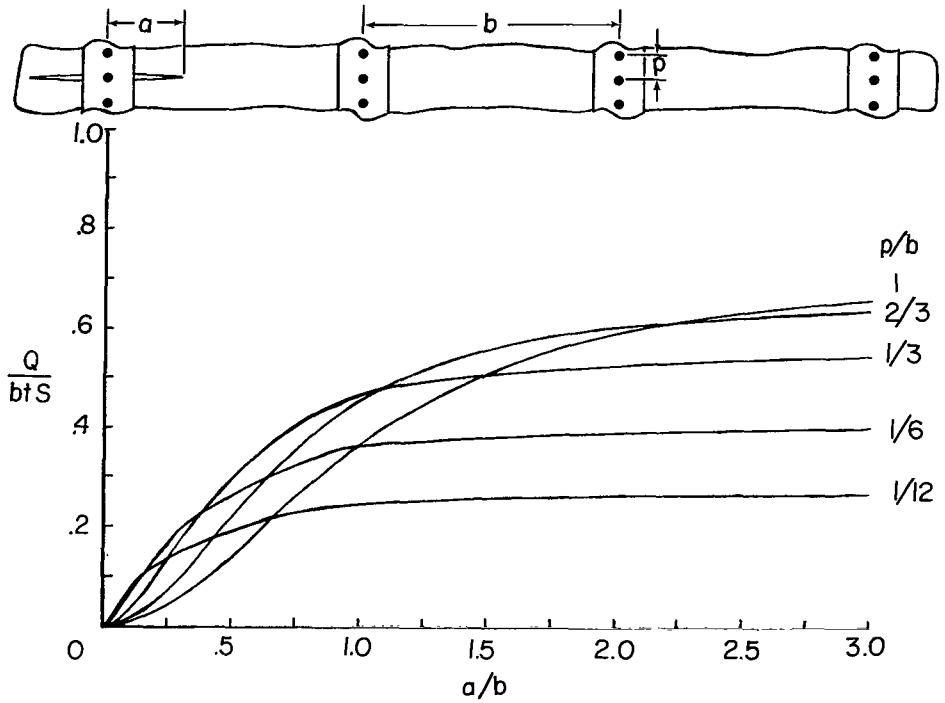

(a) Crack extending equally on both sides of stringer.

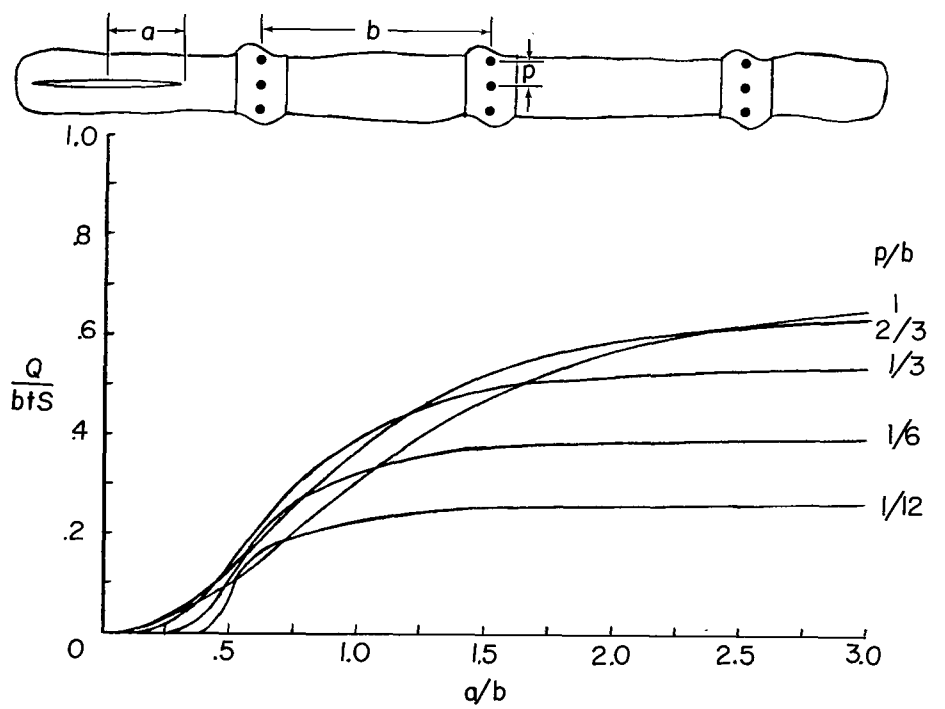

(b) Crack extending equally on both sides of point midway between two stringers.

Figure 8.- Effect of rivet spacing on relationship between rivet force and crack length for most highly loaded rivet (μ = 0.5).

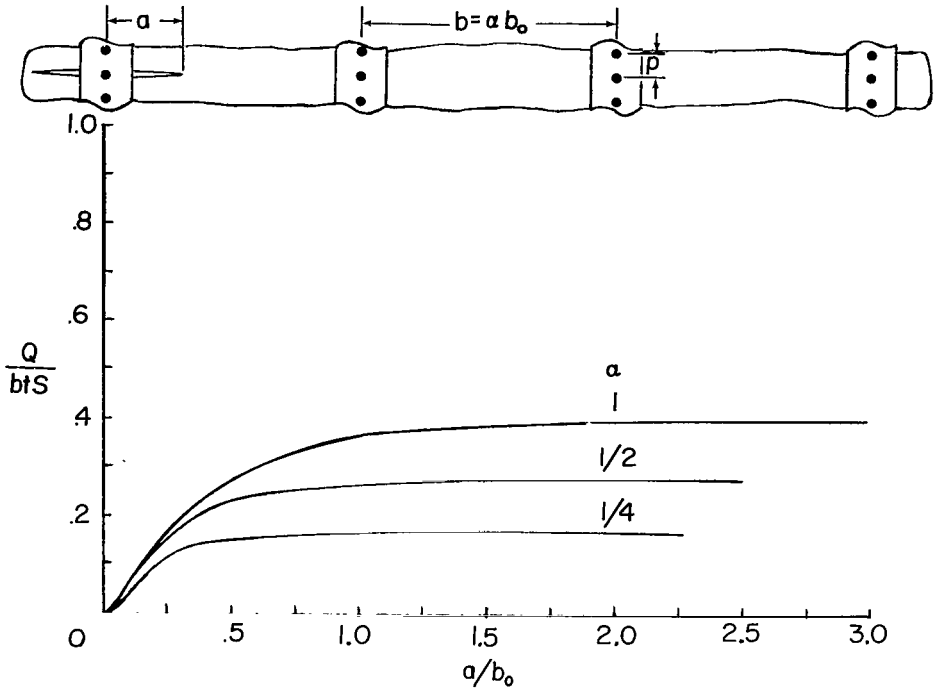

(a) Crack extending equally on both sides of stringer.

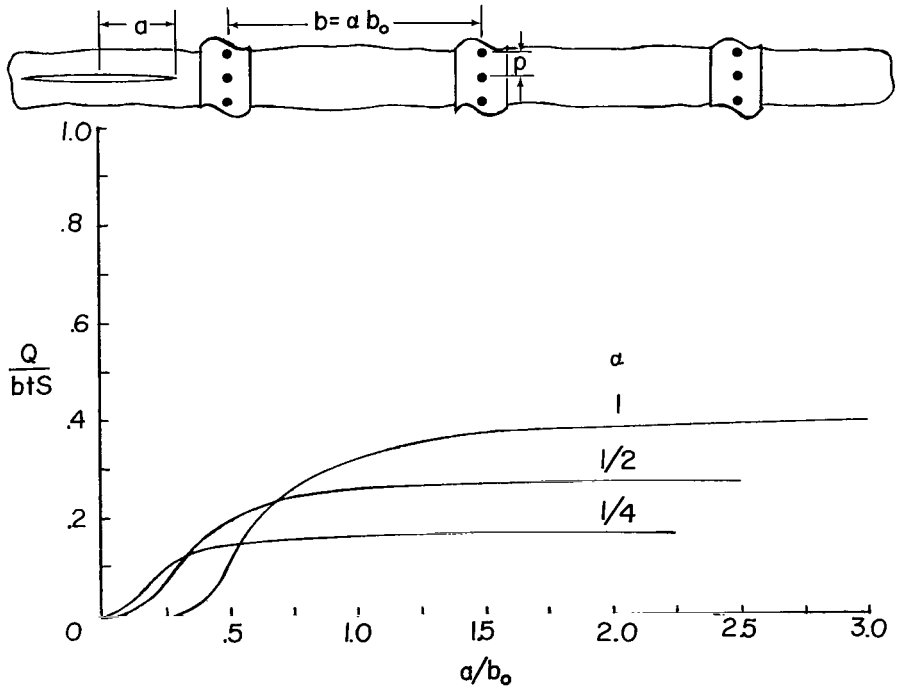

(b) Crack extending equally on both sides of point midway between two stringers.

Figure 9.- Effect of stringer spacing on relationship between rivet force and crack length for most highly loaded rivet $\left(p/b_o = 1/6 \quad \text{and} \quad \mu = 0.5\right)$.

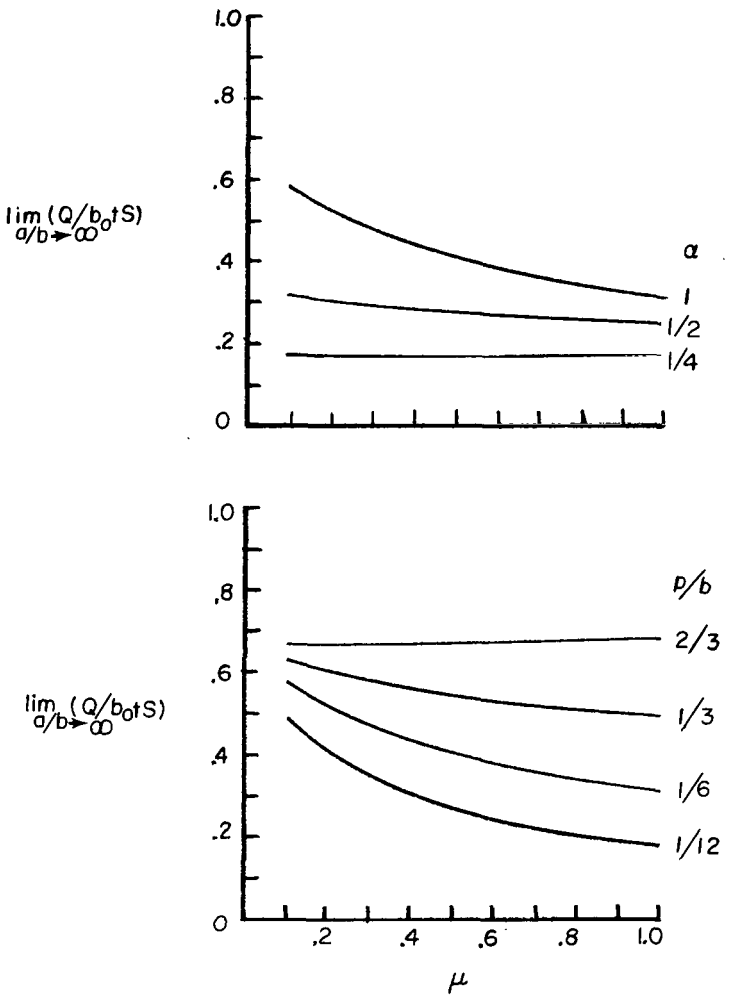

Figure 10.- Effect of stringer stiffness, stringer spacing, and rivet spacing on limiting force in most highly loaded rivet.

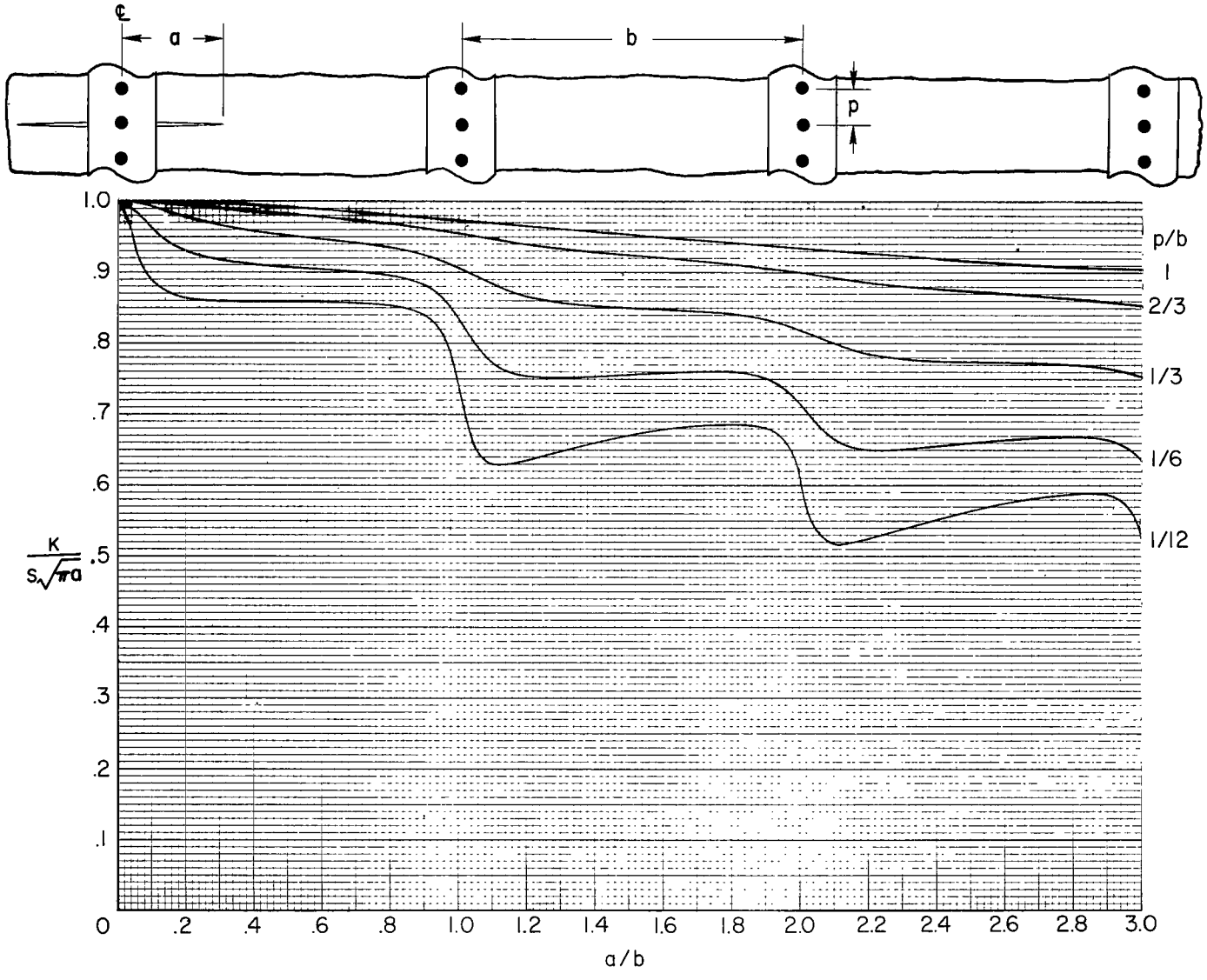

(a) $\mu = 0.05$.

Figure 11.- Stress-intensity factor for crack extending equally on both sides of stringer.

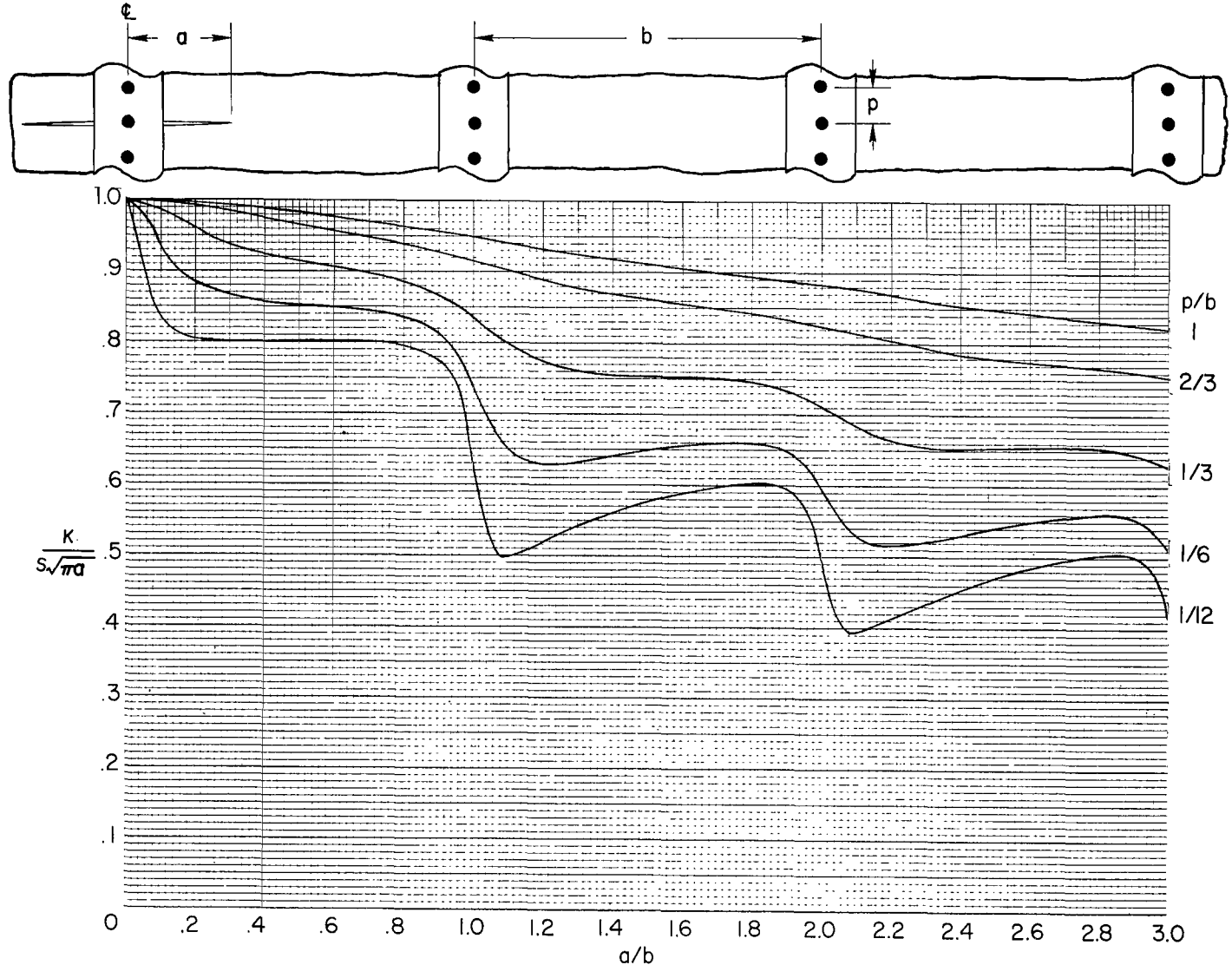

(b) $\mu = 0.10$.

Figure 11.- Continued.

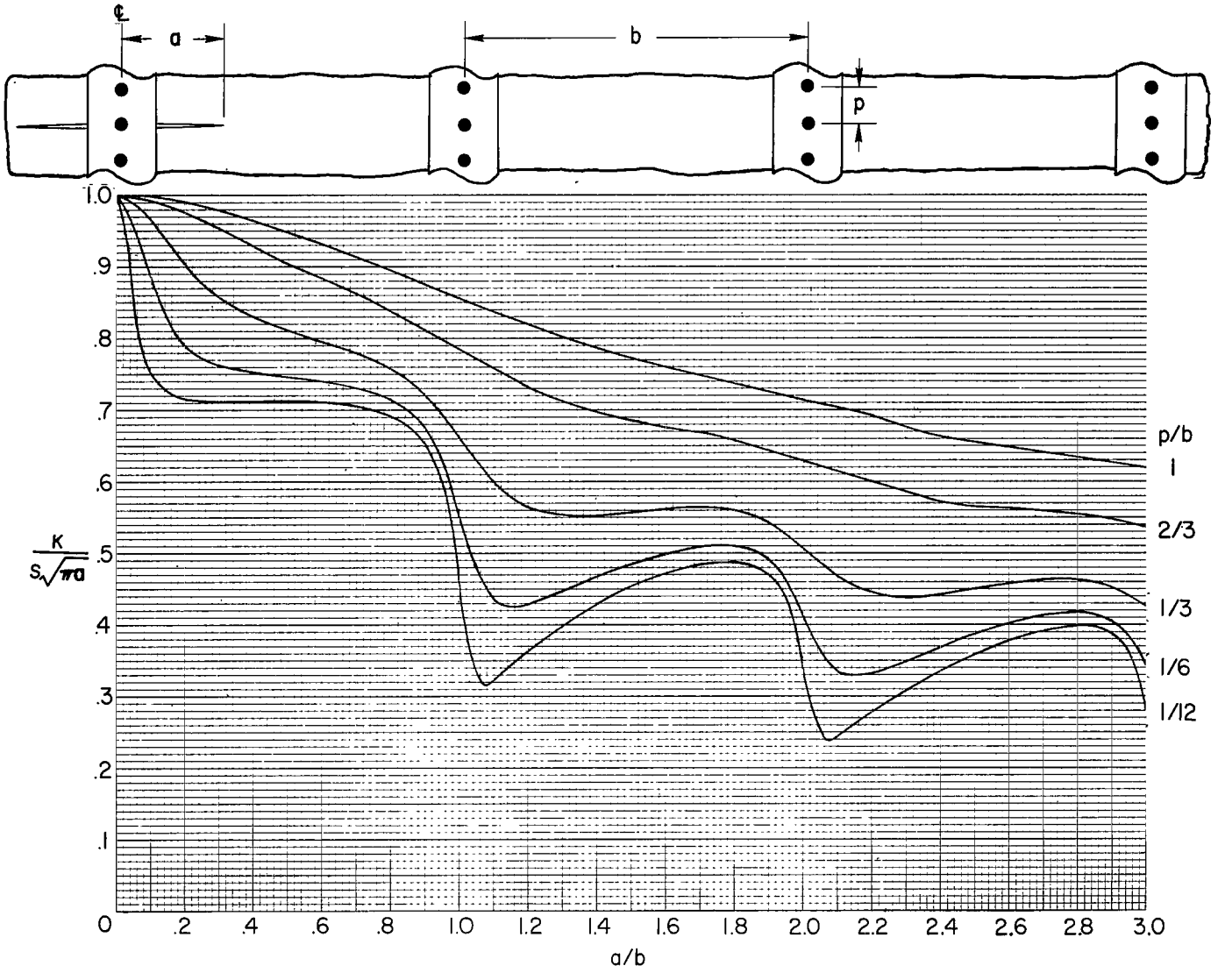

(c) $\mu = 0.30$.

Figure 11.- Continued.

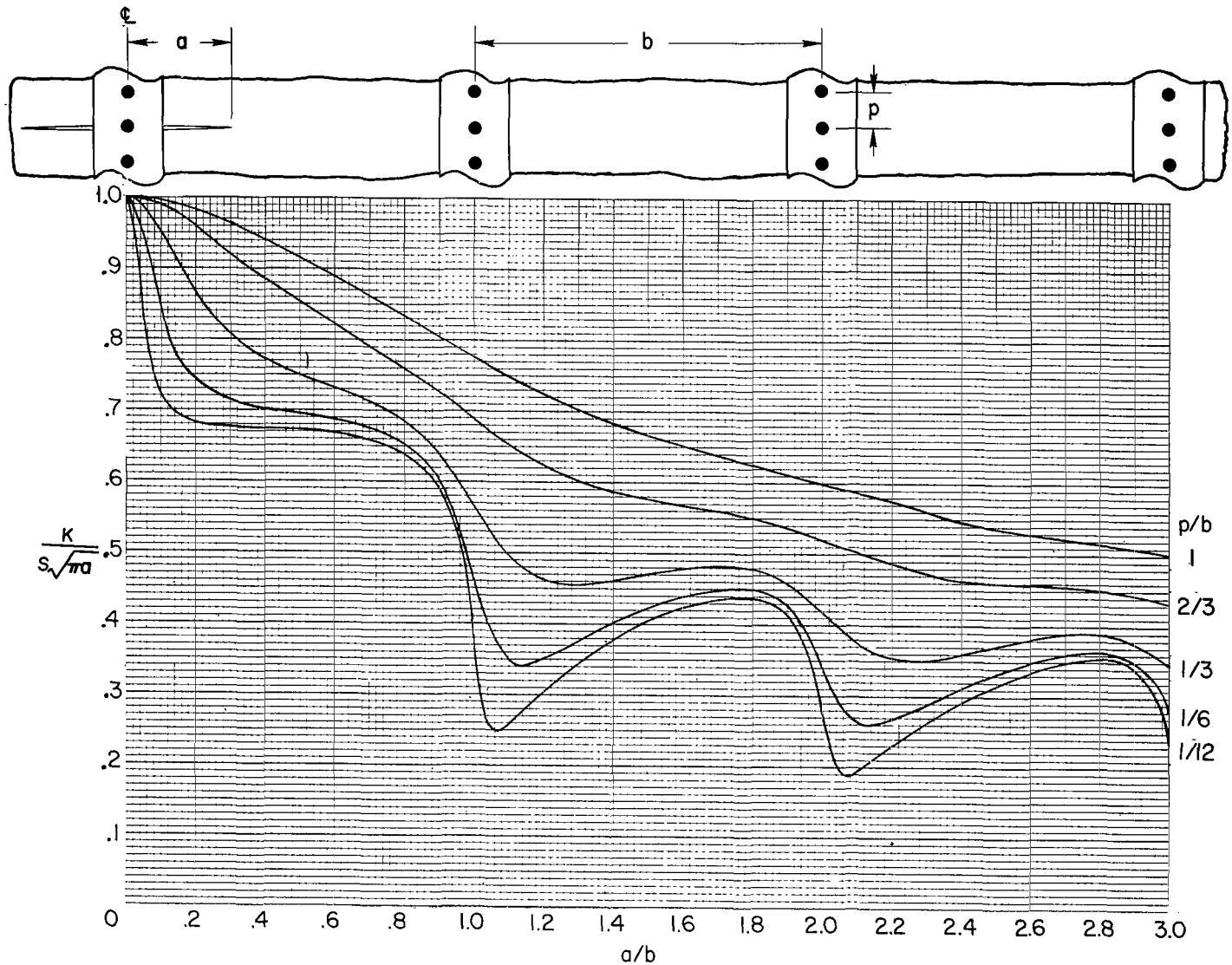

(d) $\mu = 0.50$.

Figure 11.- Continued.

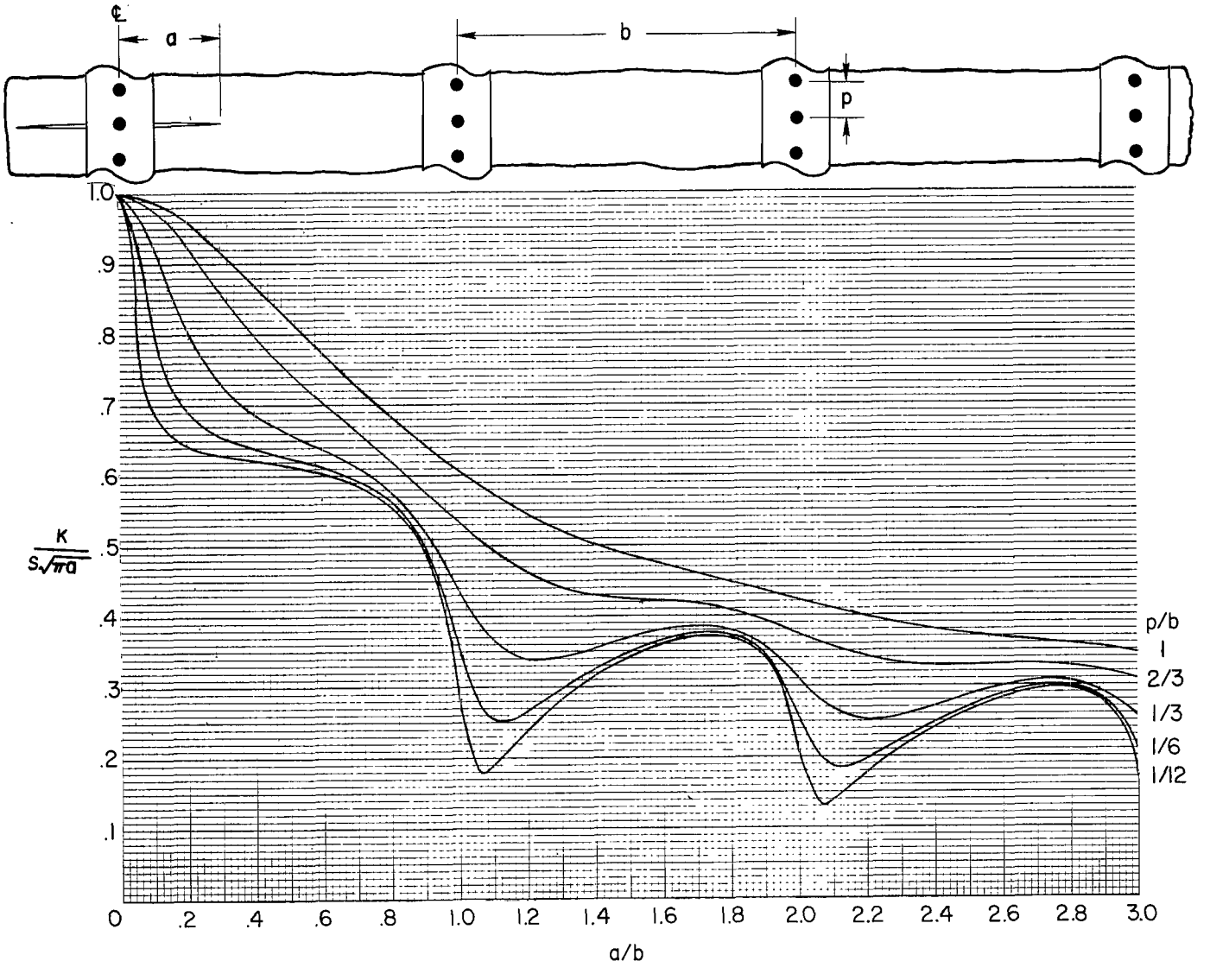

(e) $\mu = 1.00$.

Figure 11.- Concluded.

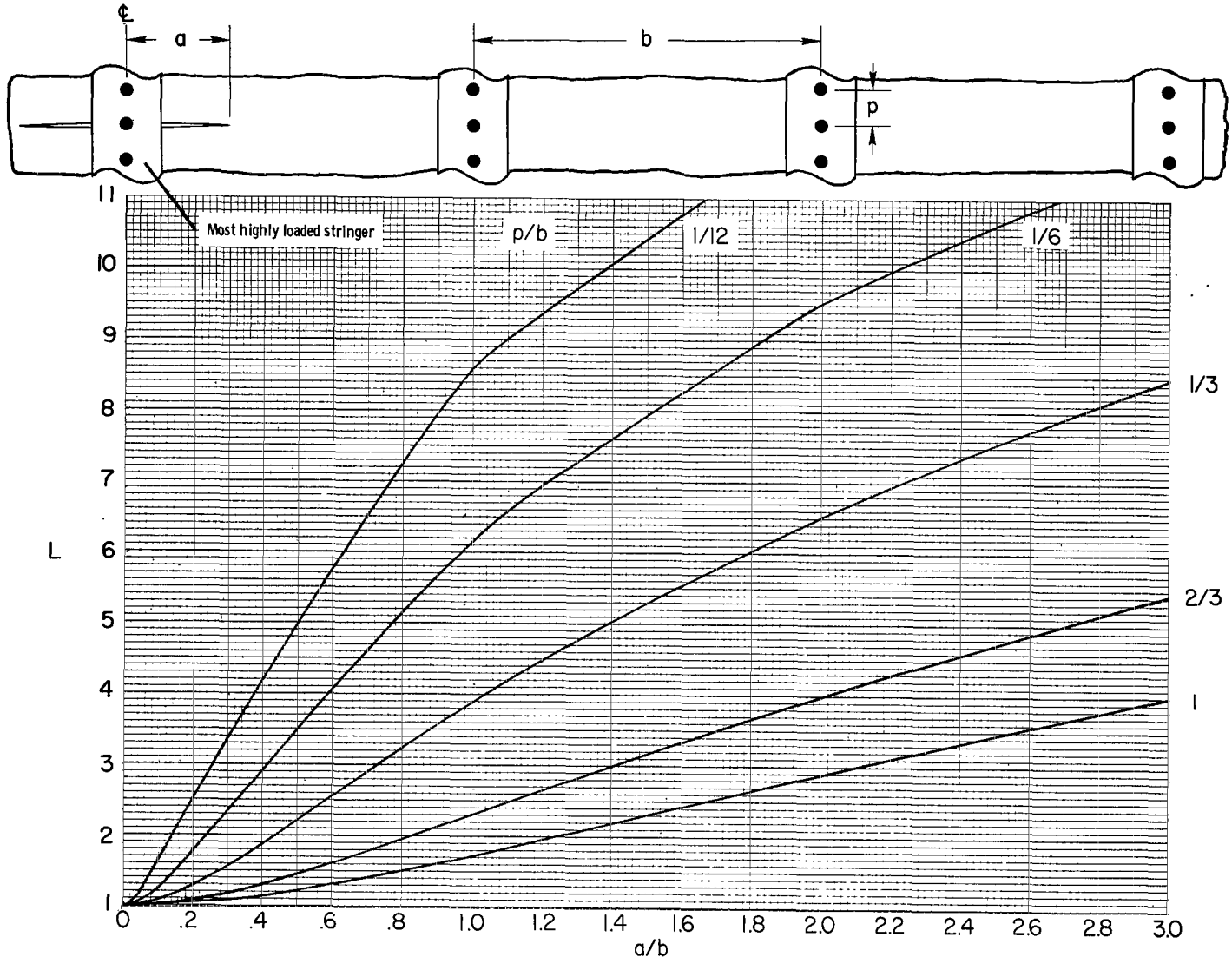

(a) $\mu = 0.05$.

Figure 12.- Stringer-load-concentration factor in most highly loaded stringer for crack extending equally on both sides of stringer. (Scale of ordinate is different for some parts of this figure.)

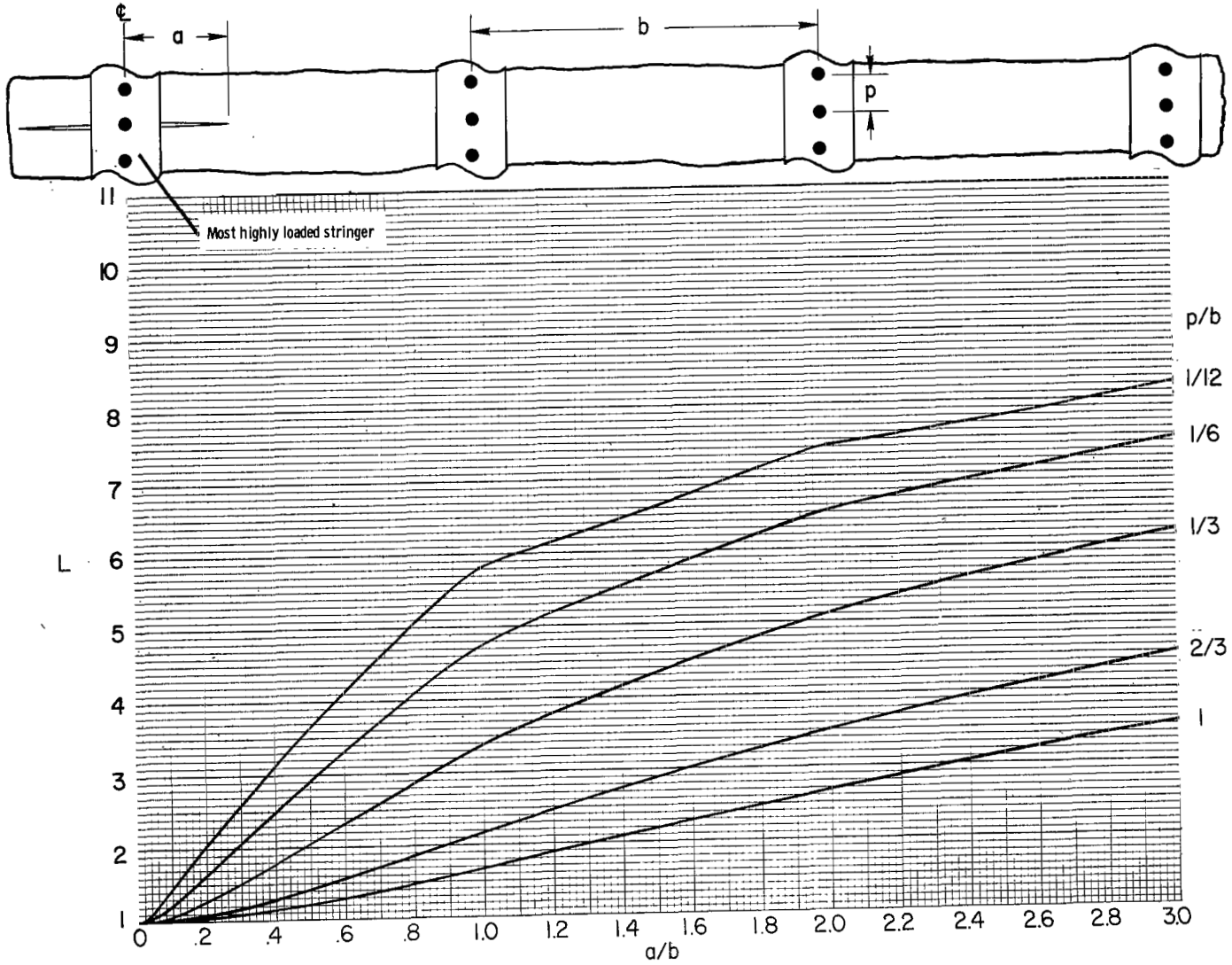

(b) $\mu = 0.10$.

Figure 12.- Continued.

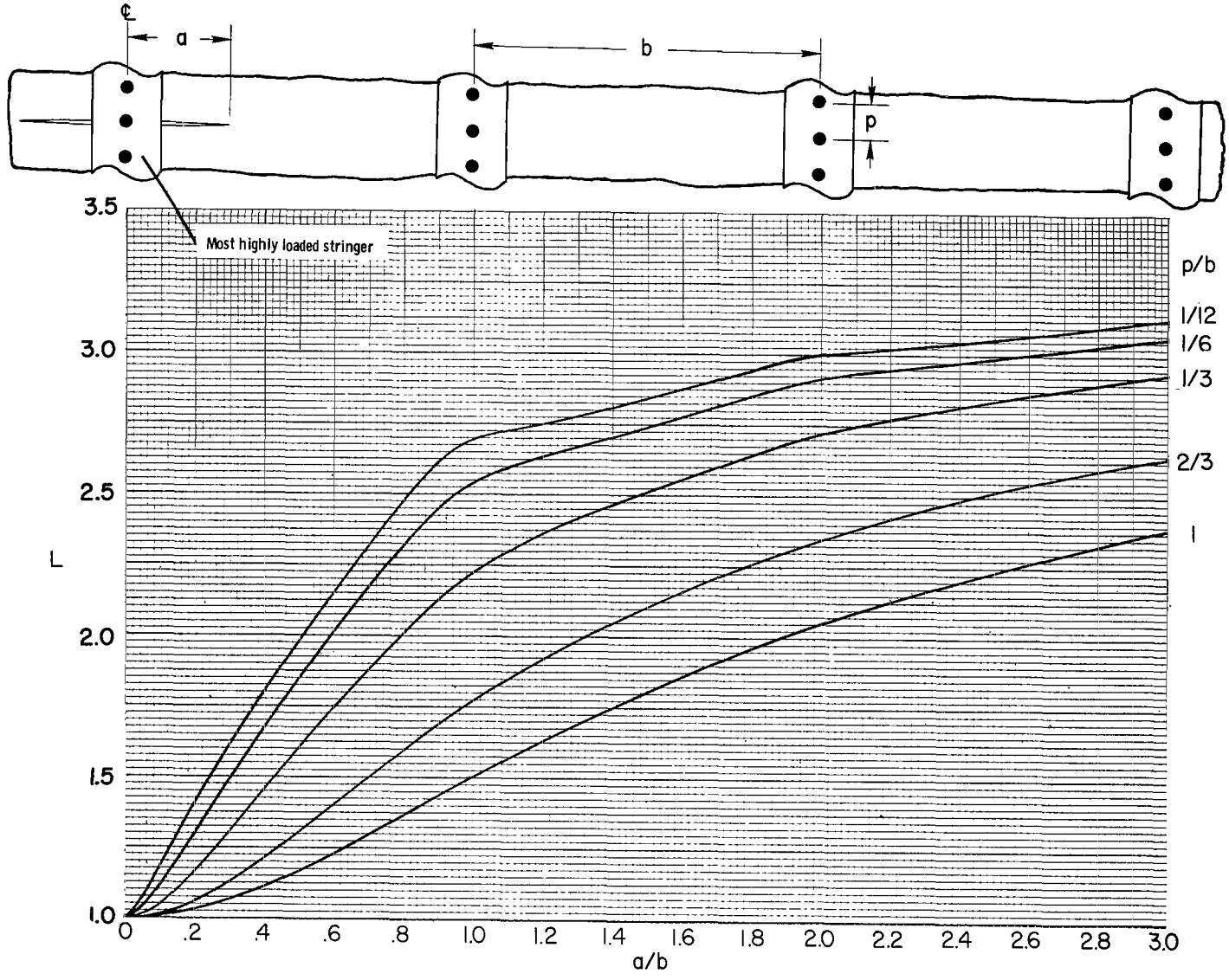

(c) $\mu = 0.30$.

Figure 12.- Continued.

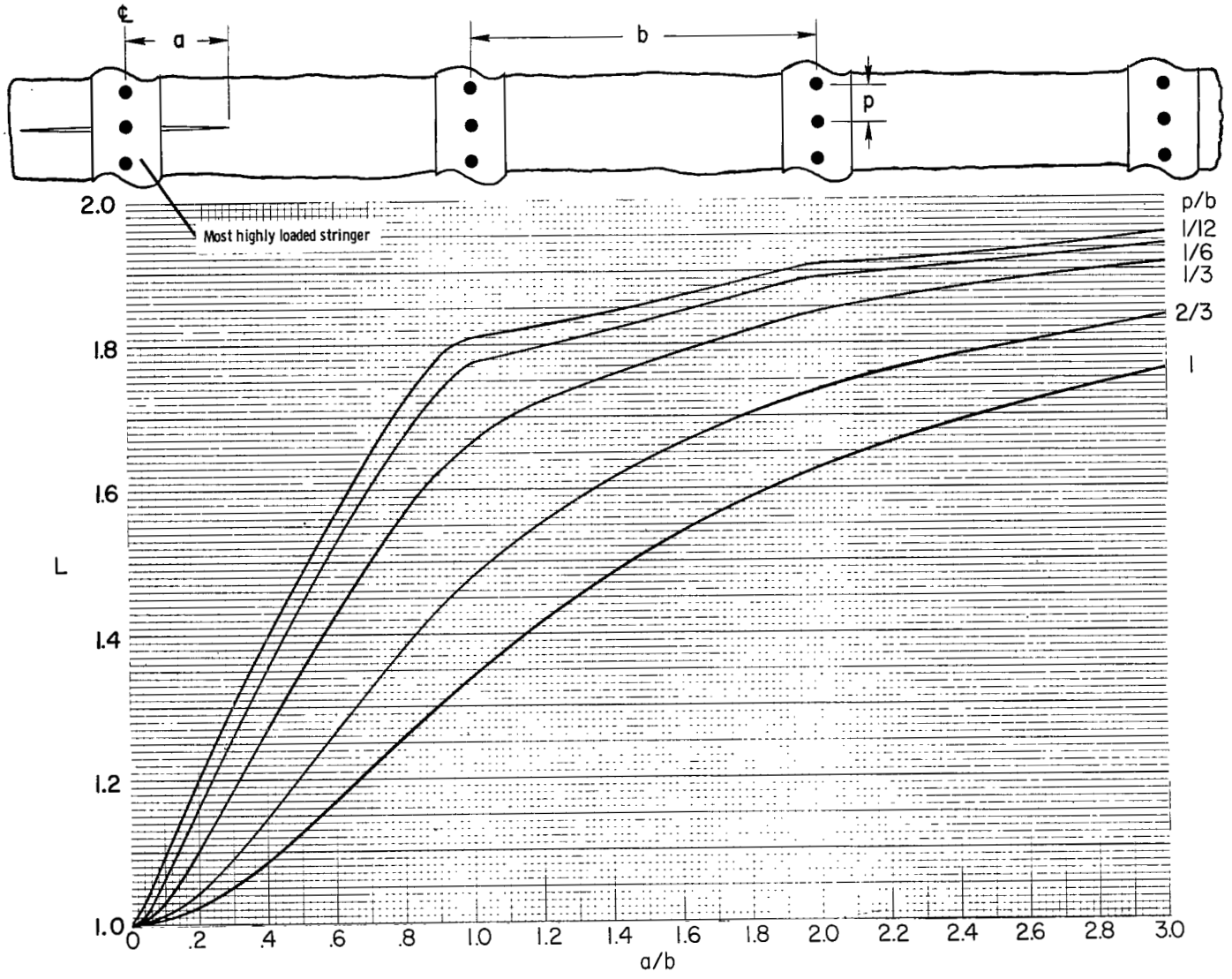

(d) $\mu = 0.50$.

Figure 12.- Concluded.

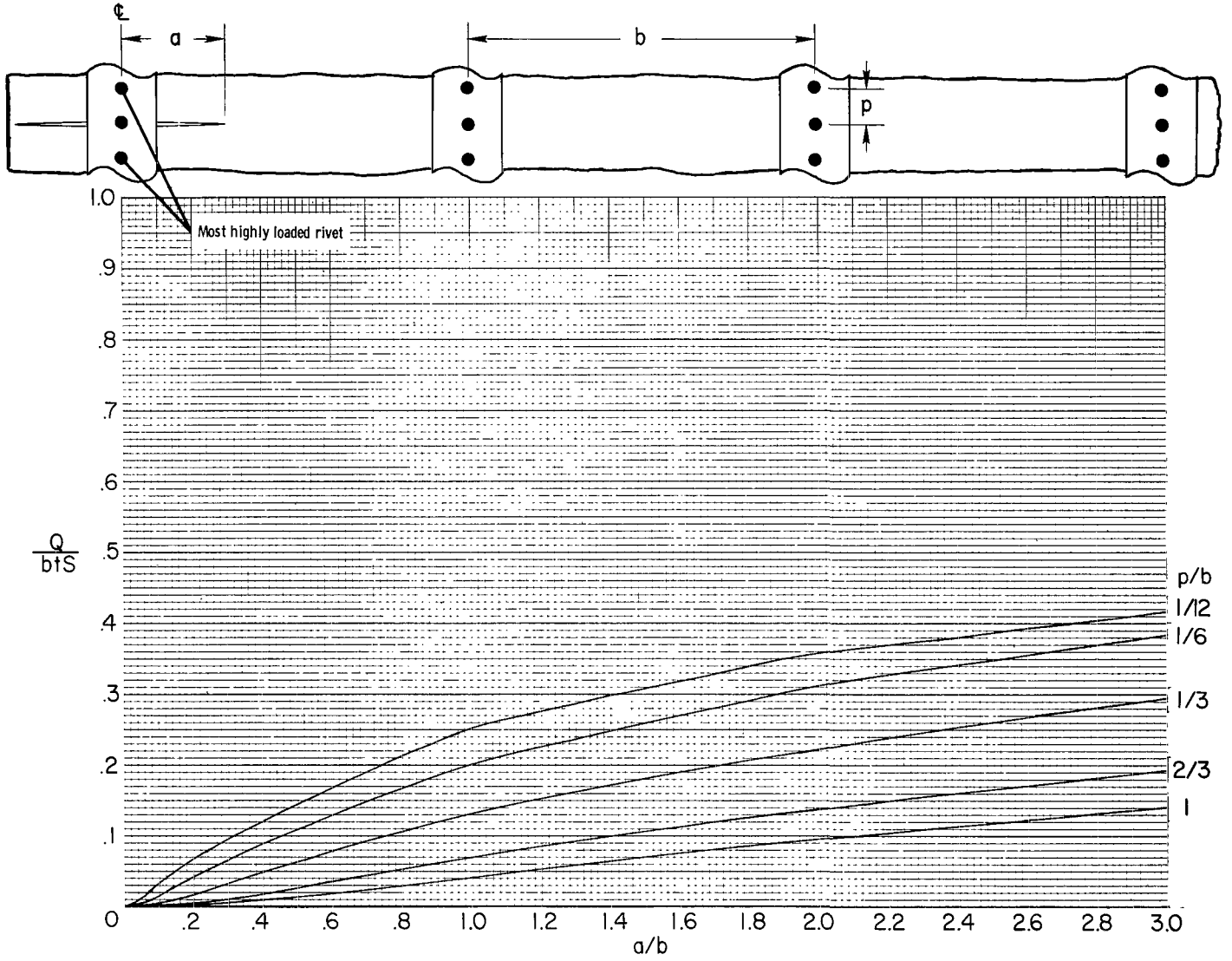

(a) $\mu = 0.05$.

Figure 13.- Force in most highly loaded rivet for crack extending equally on both sides of stringer.

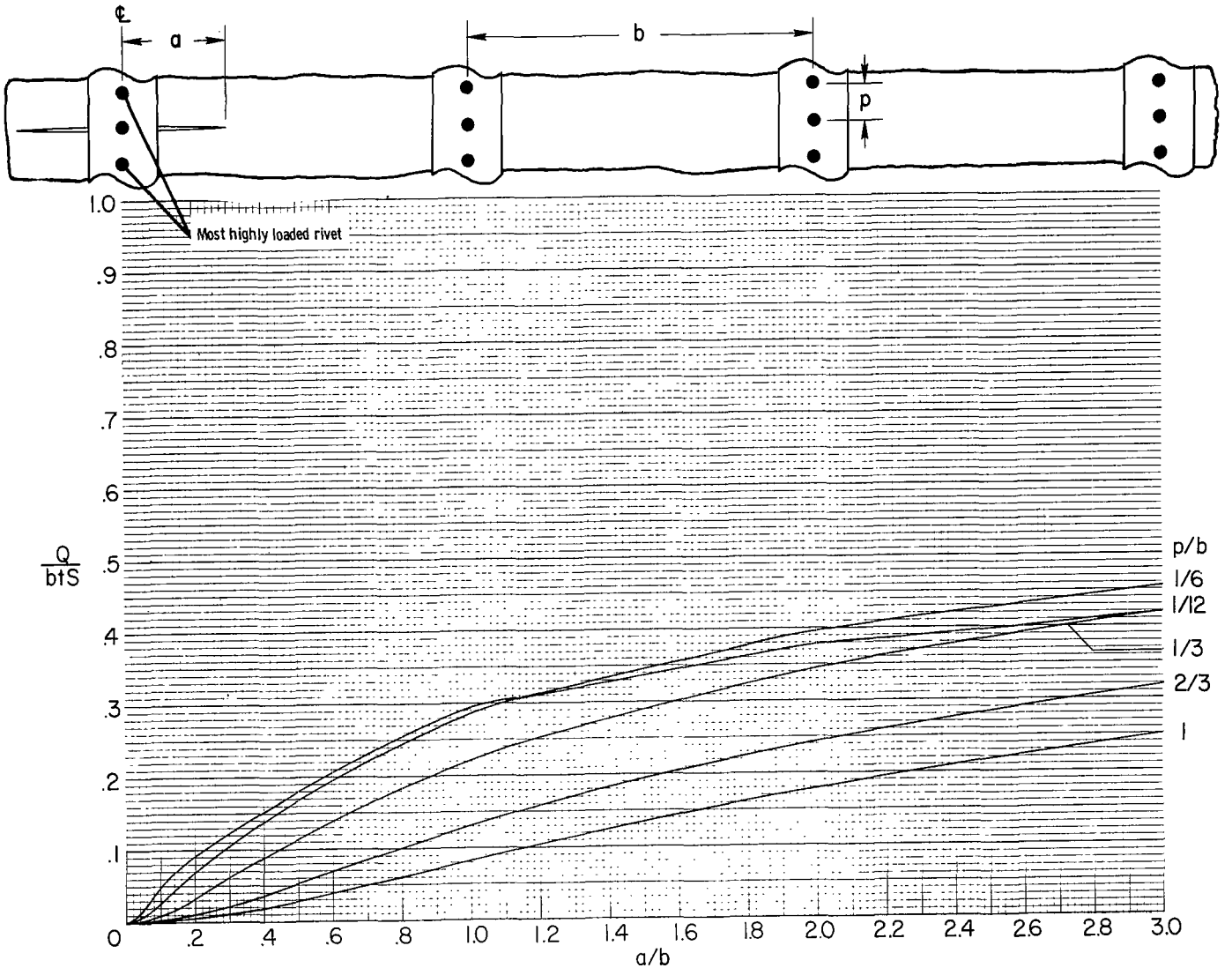

(b) $\mu = 0.10$.

Figure 13.- Continued.

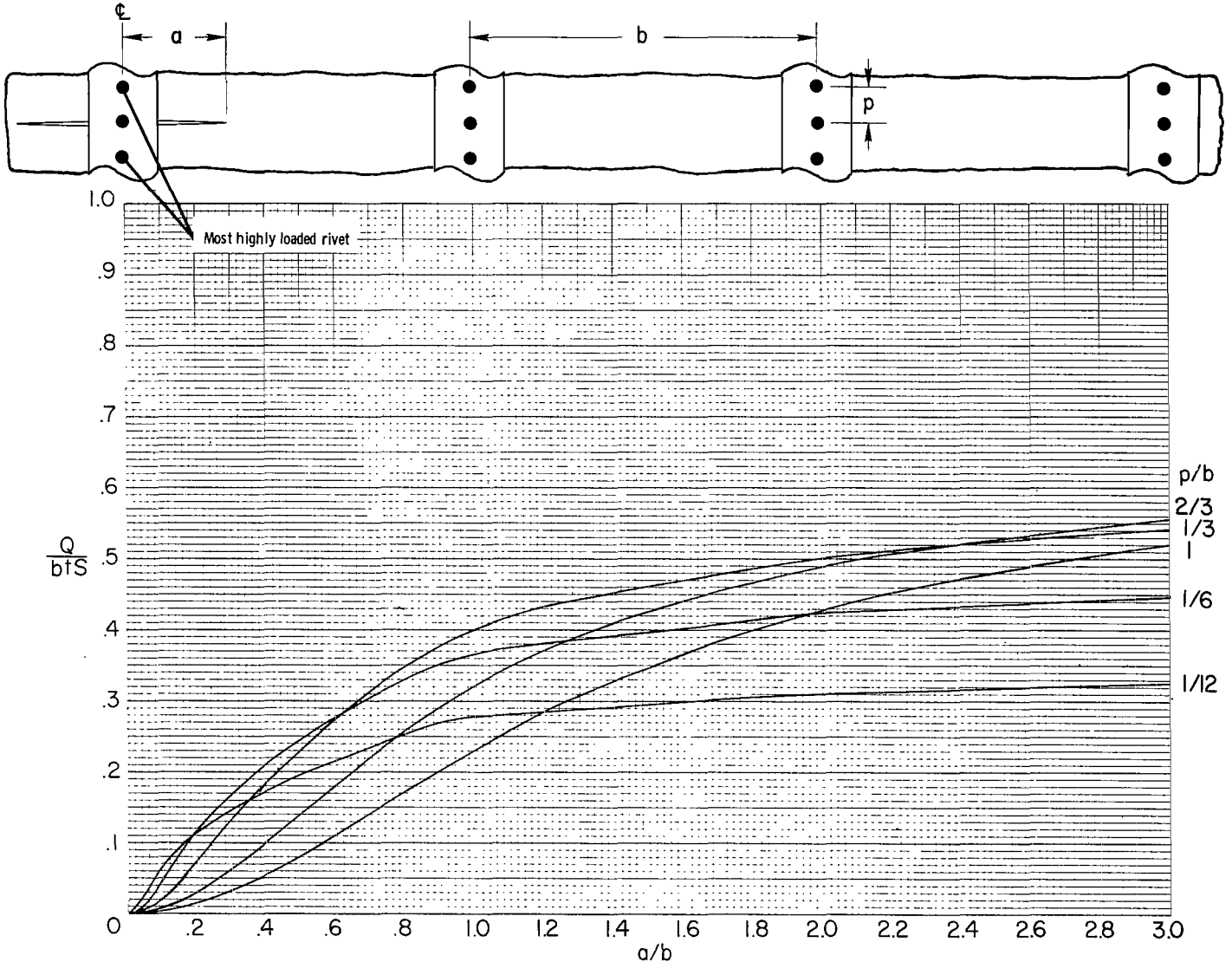

(c) $\mu = 0.30$.

Figure 13.- Continued.

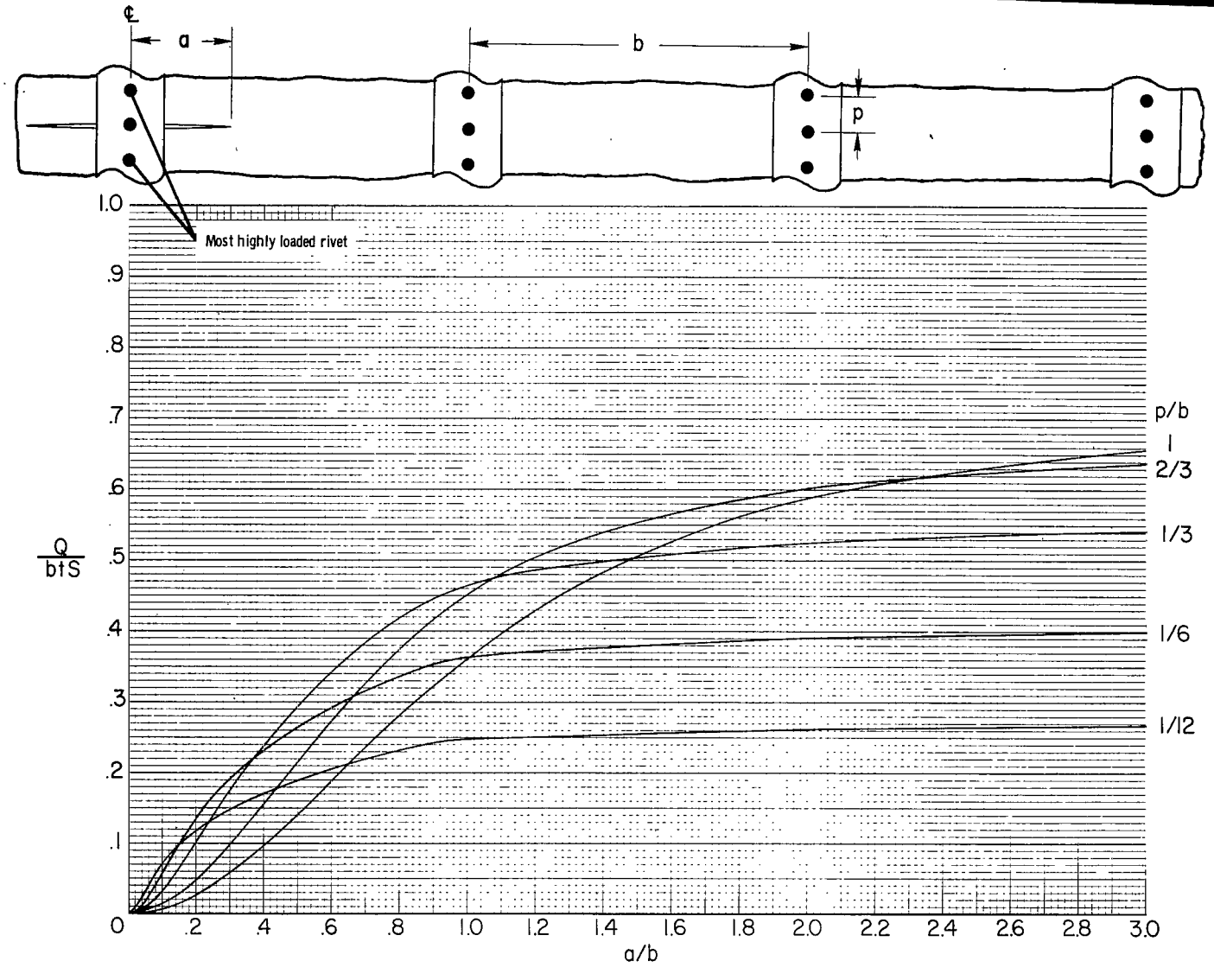

(d) $\mu = 0.50$.

Figure 13.- Continued.

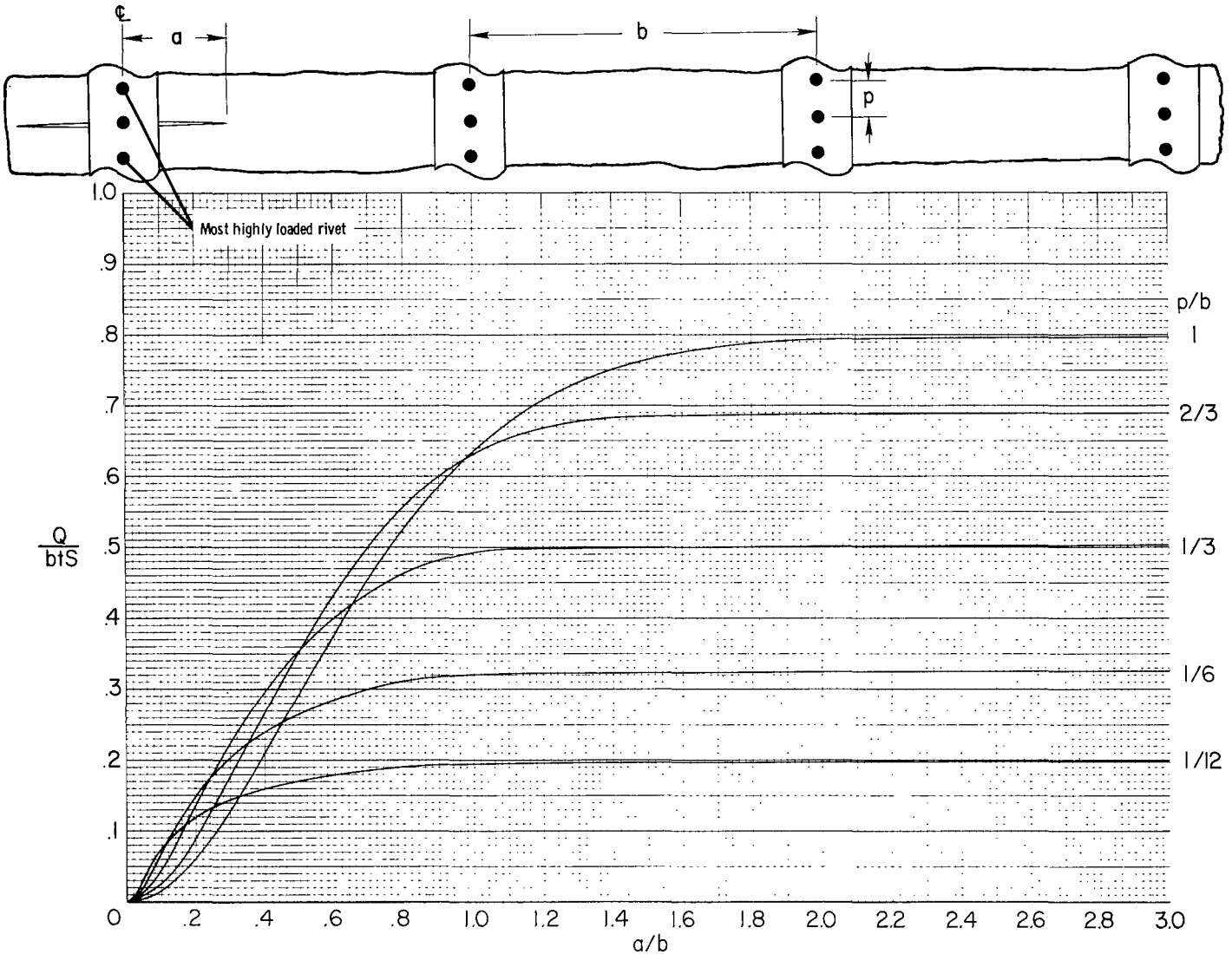

(e) $\mu = 1.00$.

Figure 13.- Concluded.

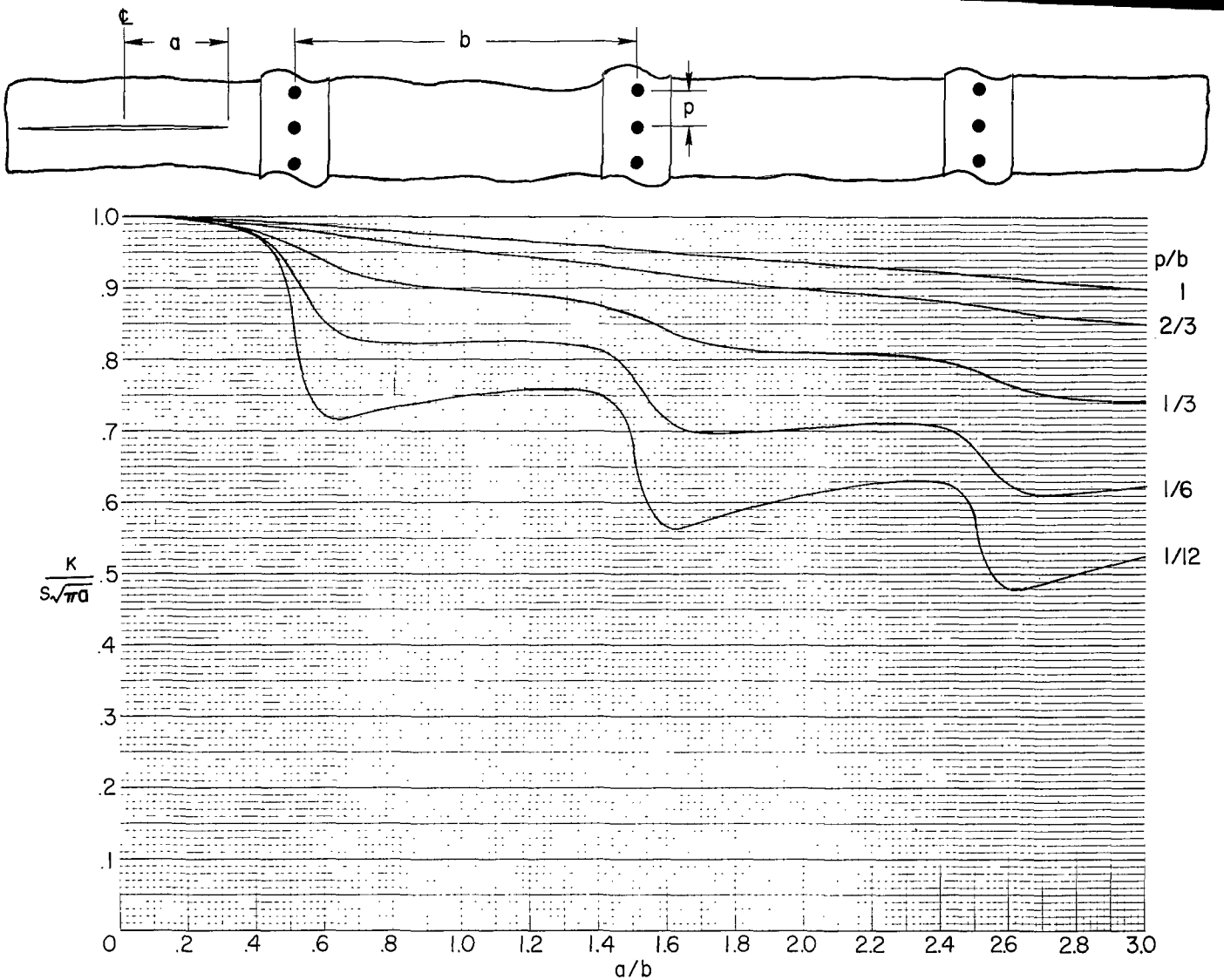

(a) $\mu = 0.05$.

Figure 14.- Stress-intensity factor for crack extending equally on both sides of point midway between two stringers.

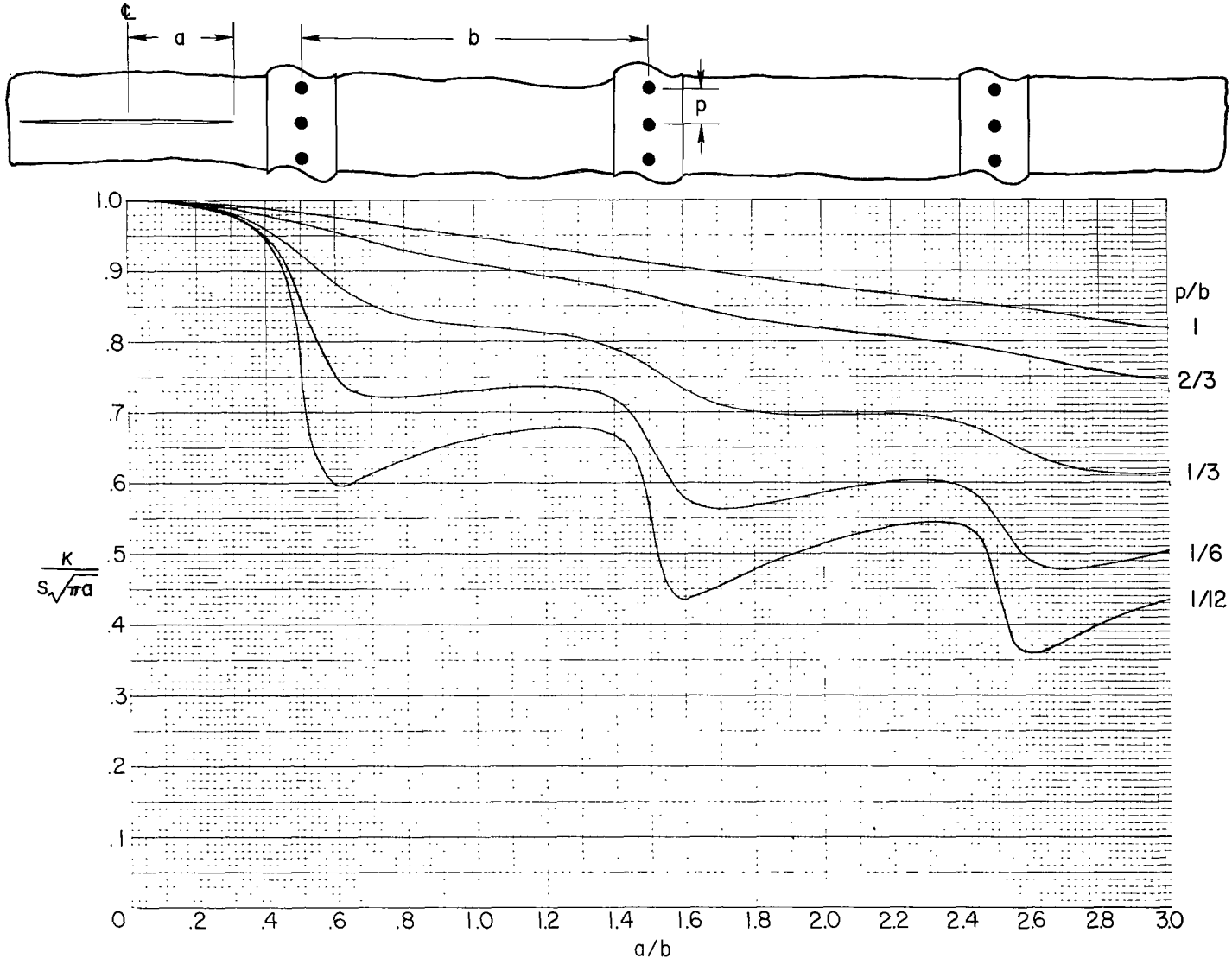

(b) $\mu = 0.10$.

Figure 14.- Continued.

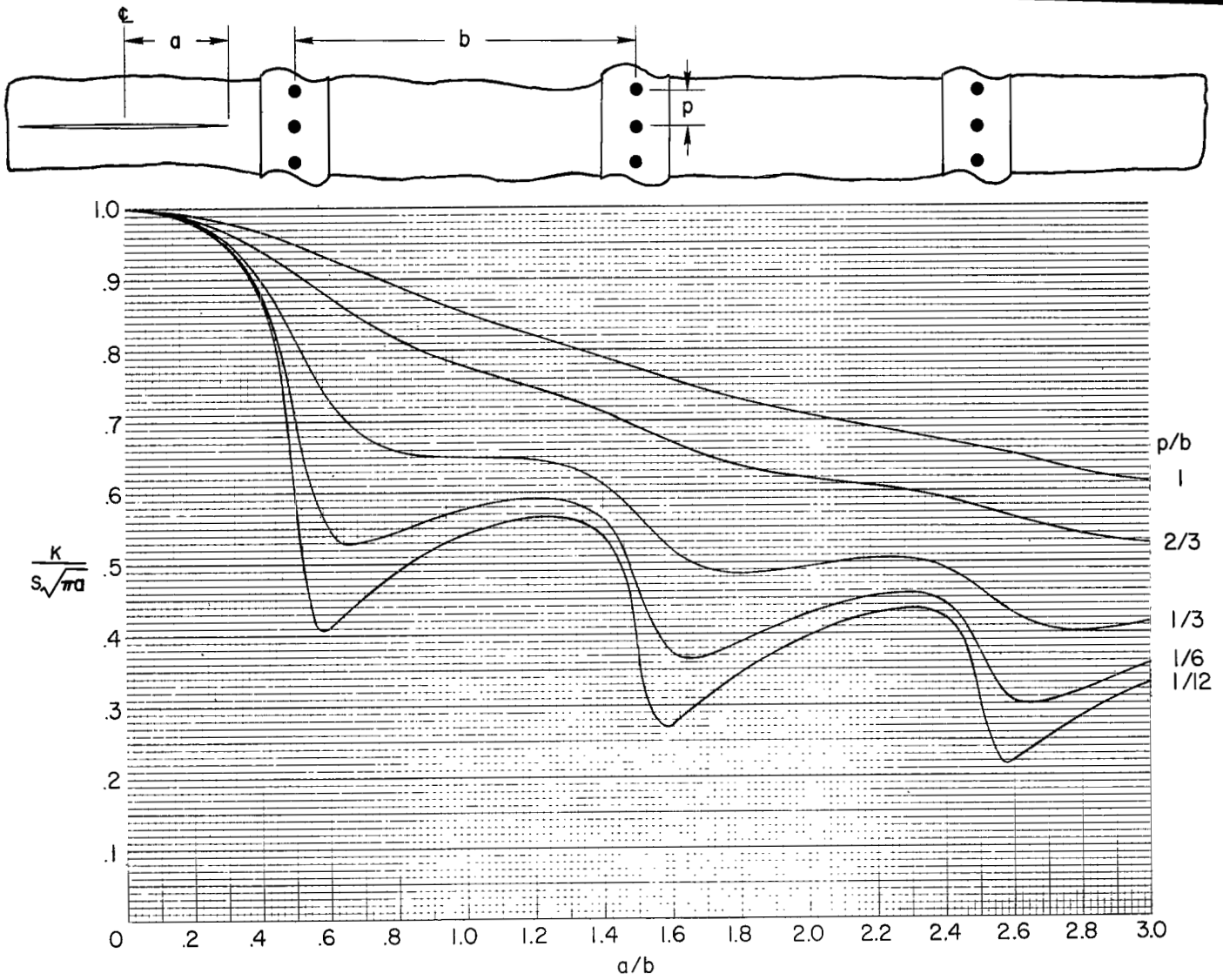

(c) $\mu = 0.30$.

Figure 14.- Continued.

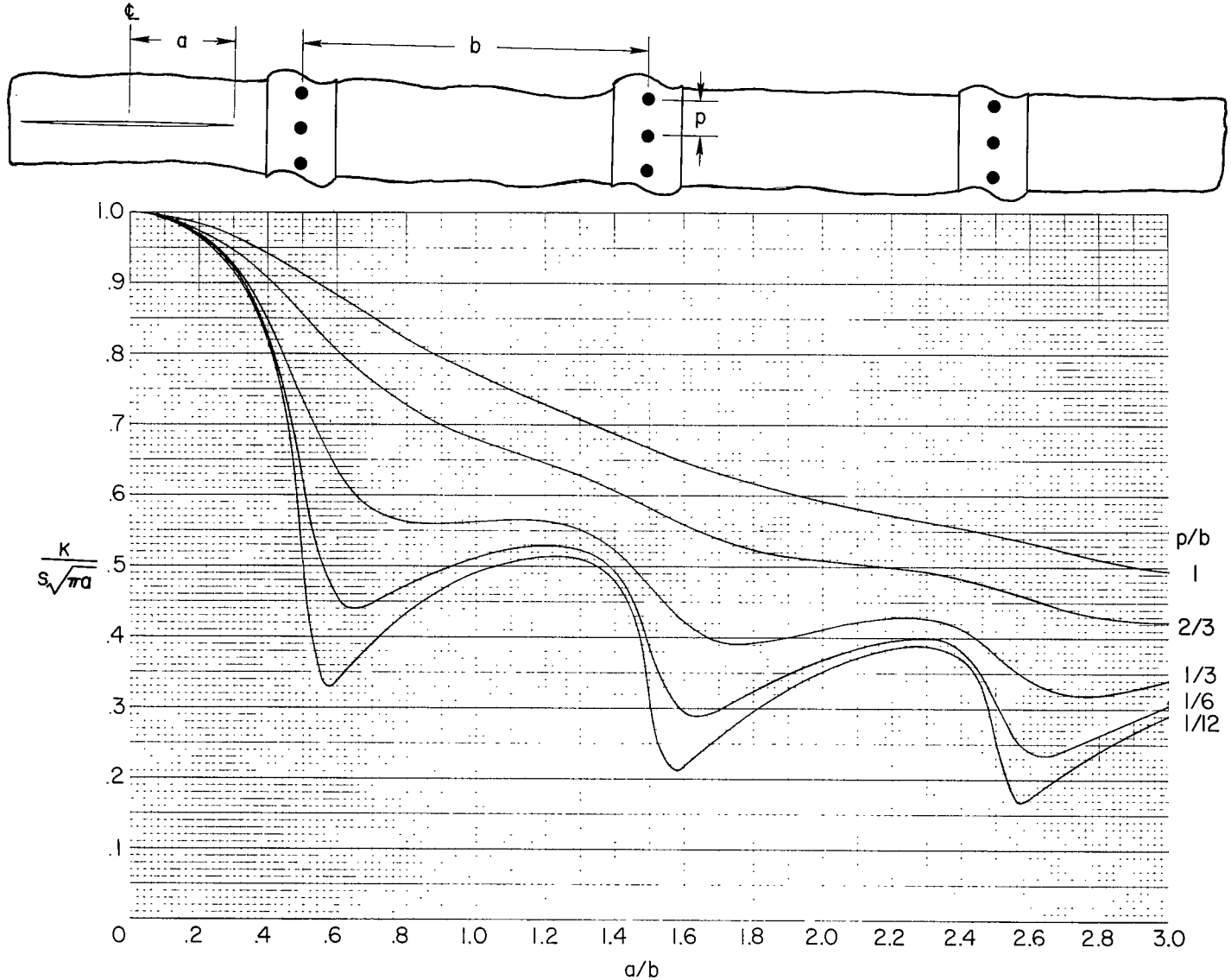

(d) $\mu = 0.50$.

Figure 14.- Continued.

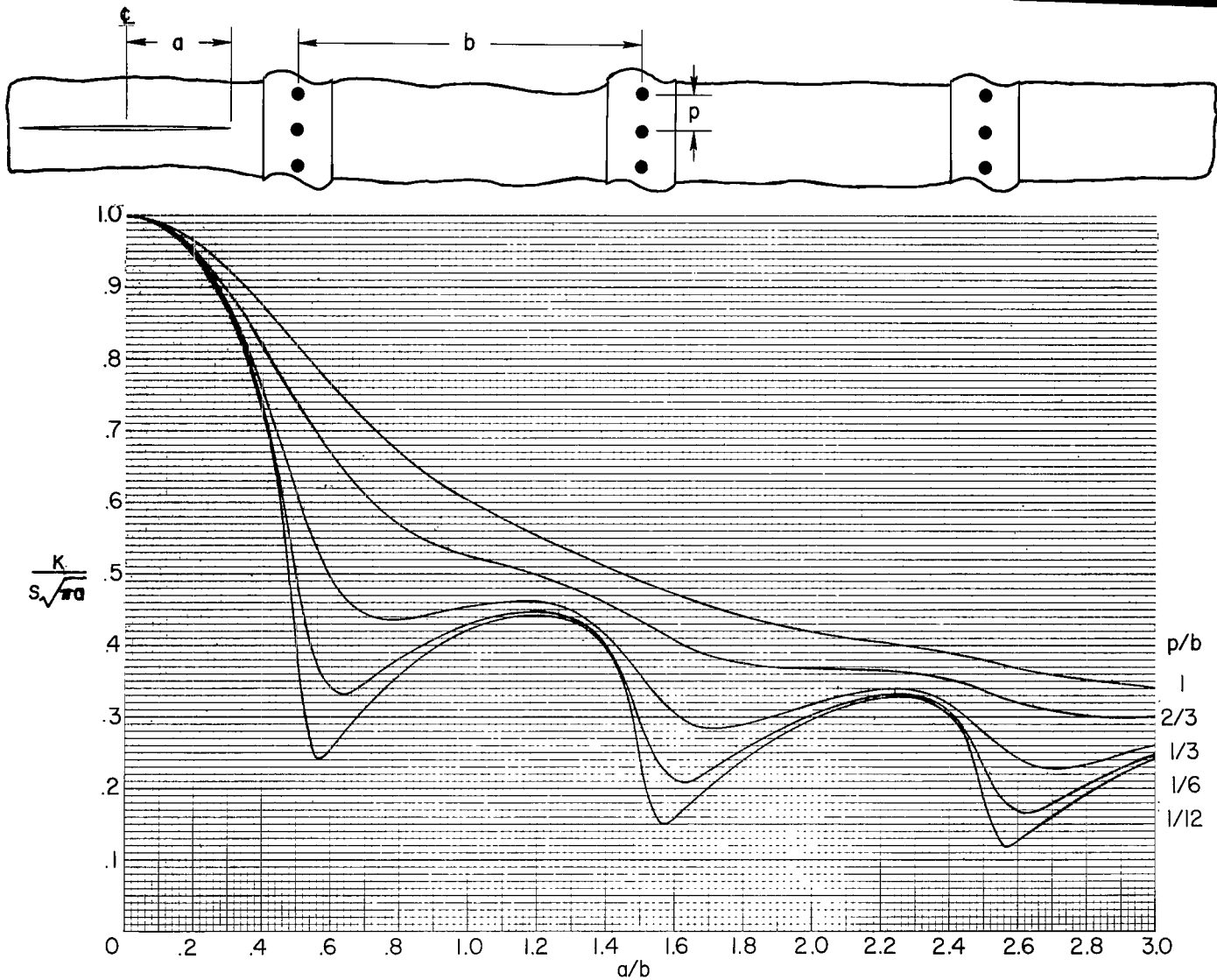

(e) $\mu = 1.00$.

Figure 14.- Concluded.

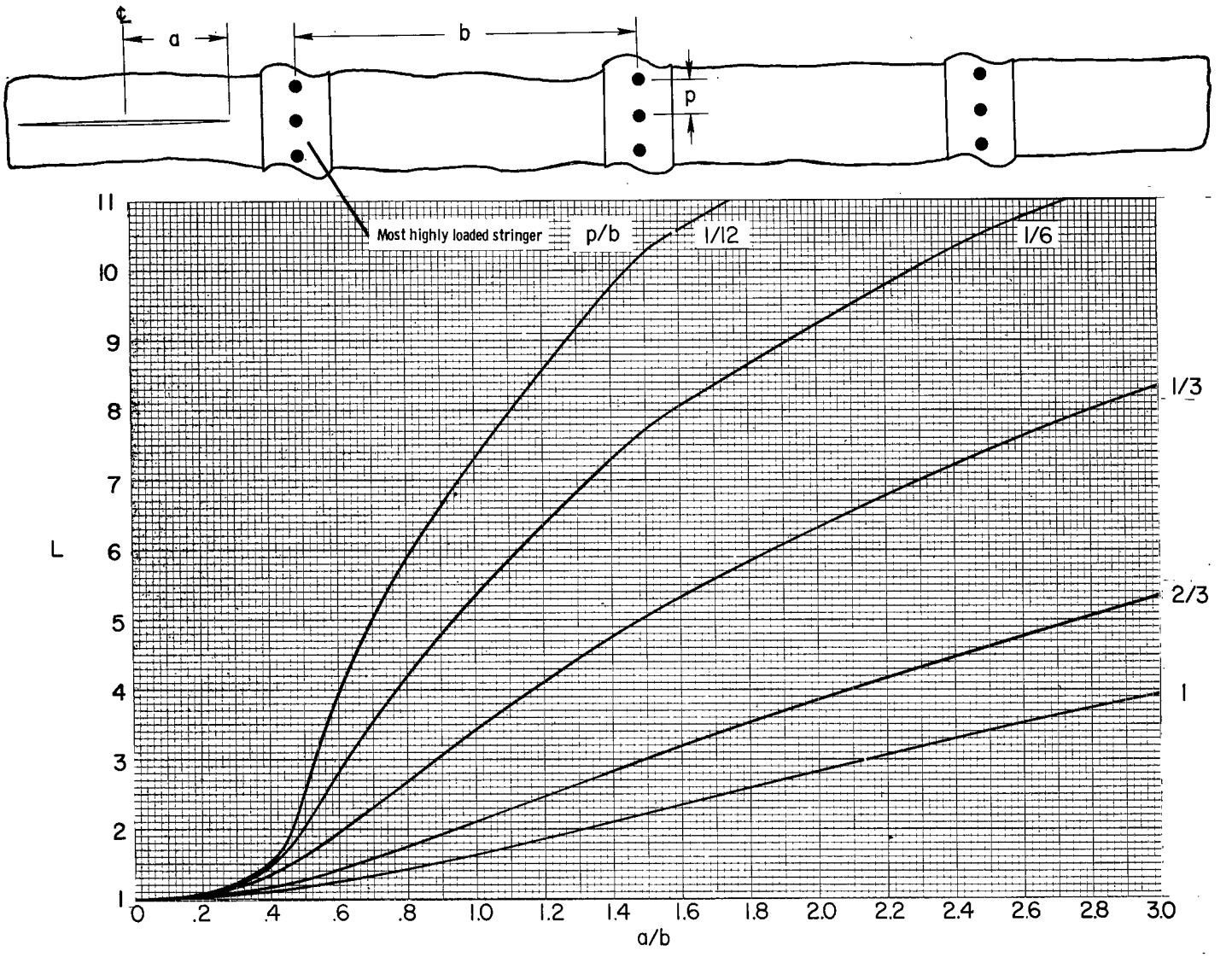

(a) $\mu = 0.05$.

Figure 15.- Stringer-load-concentration factor in most highly loaded stringer for crack extending equally on both sides of point midway between two stringers. (Scale of ordinate is different for some parts of this figure.)

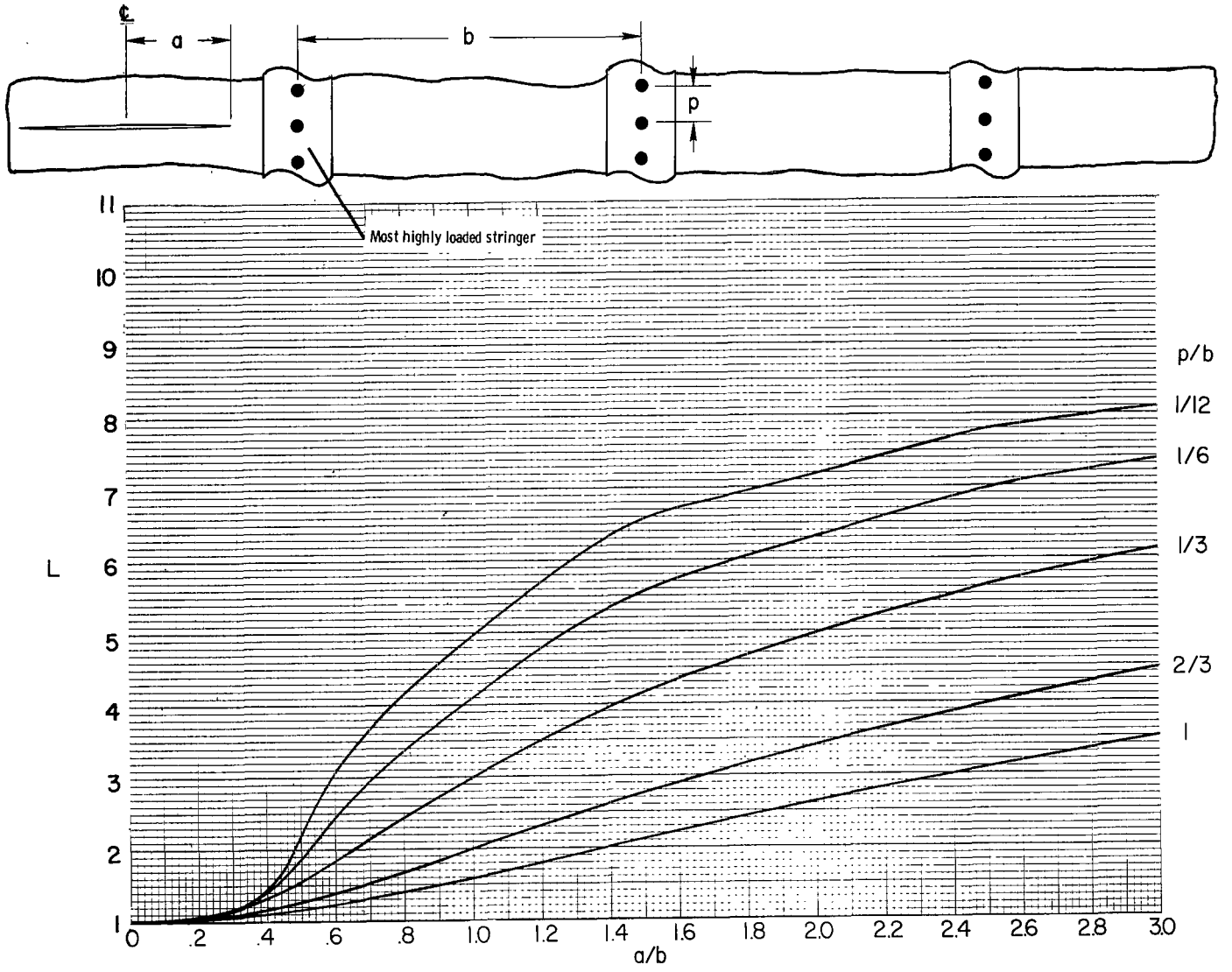

(b) $\mu = 0.10$.

Figure 15.- Continued.

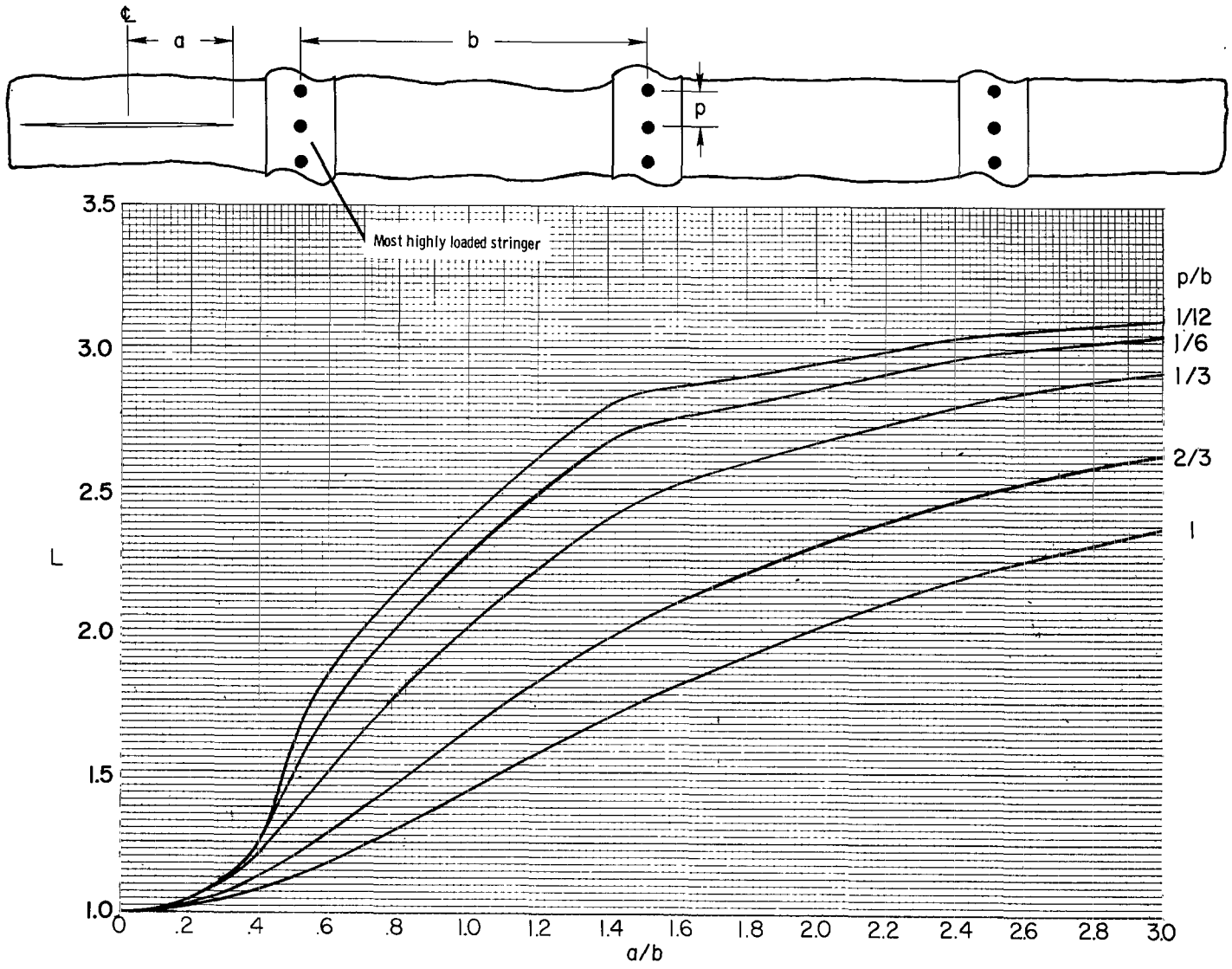

(c) $\mu = 0.30$.

Figure 15.- Continued.

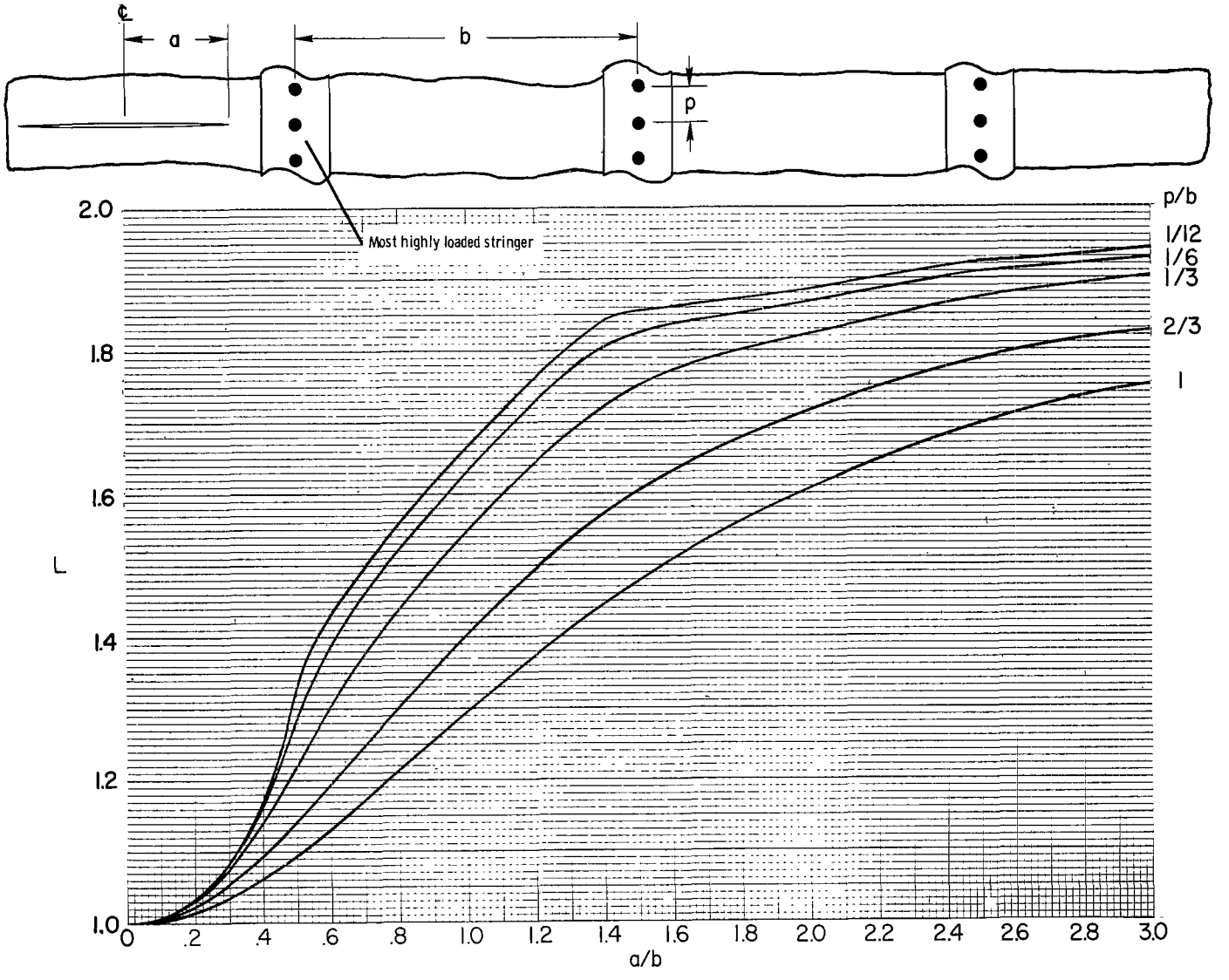

(d) $\mu = 0.50$.

Figure 15.- Concluded.

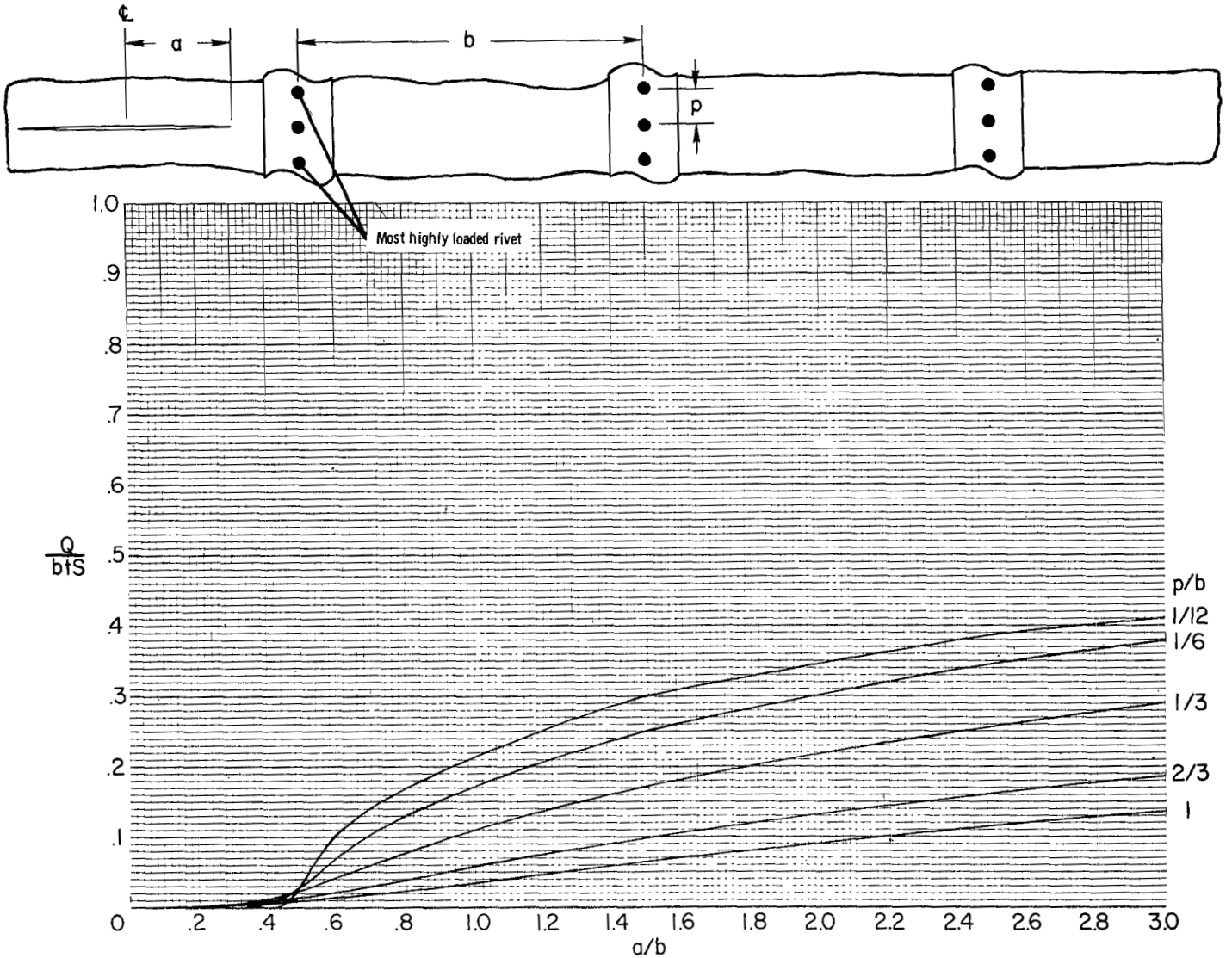

(a) $\mu = 0.05$.

Figure 16.- Force in most highly loaded rivet for crack extending equally on both sides of point midway between two stringers.

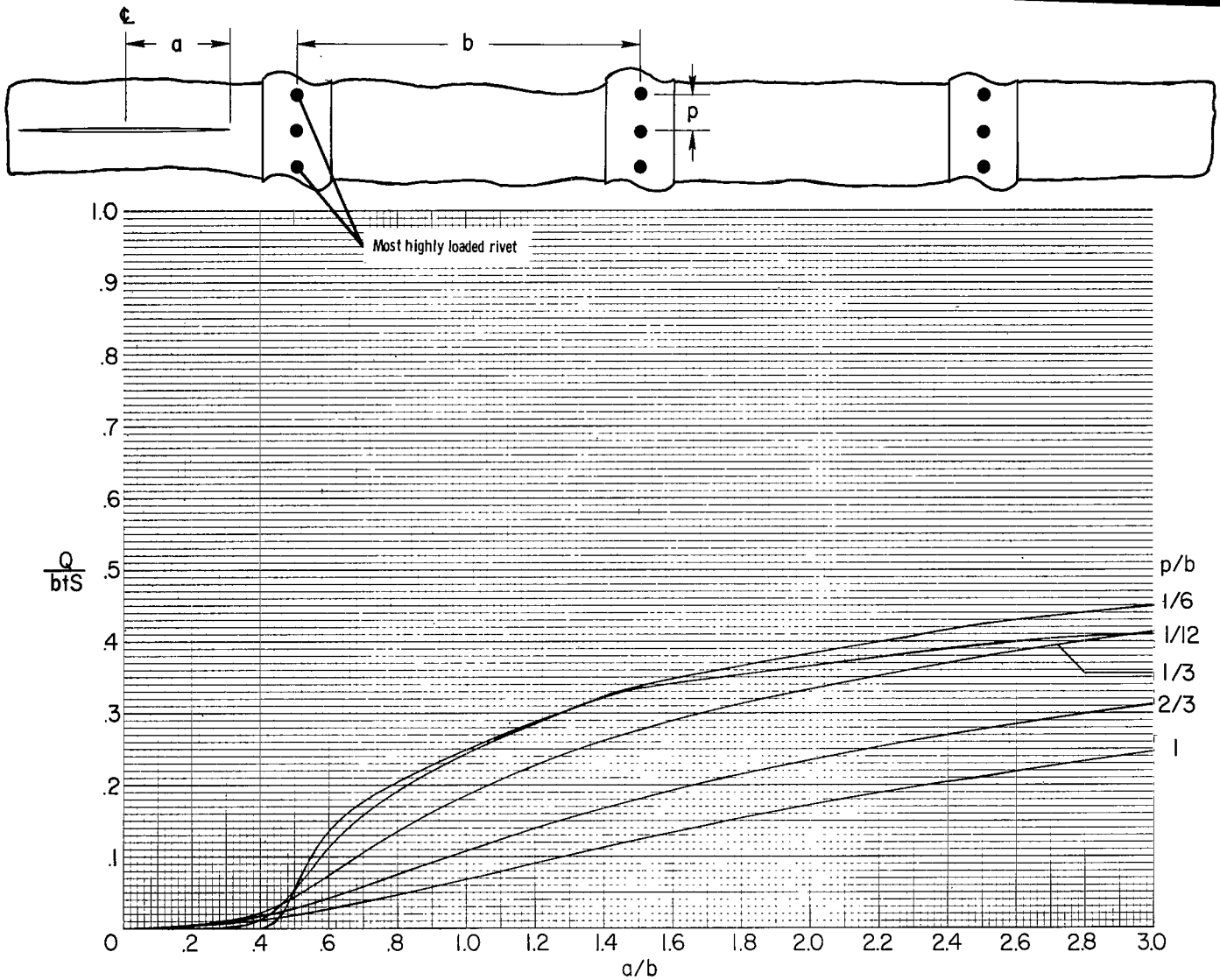

(b) $\mu = 0.10$.

Figure 16.- Continued.

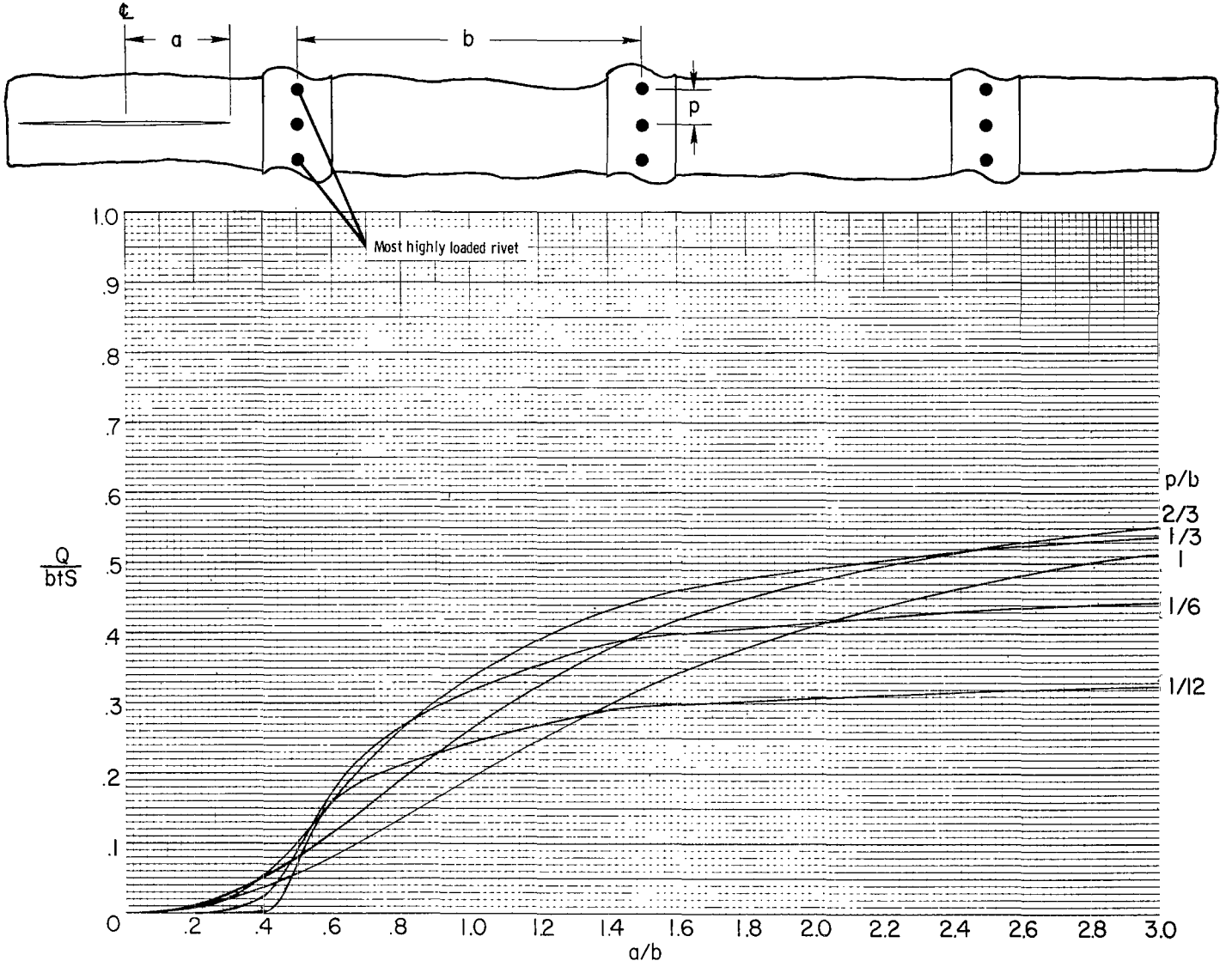

(c) $\mu = 0.30$.

Figure 16.- Continued.

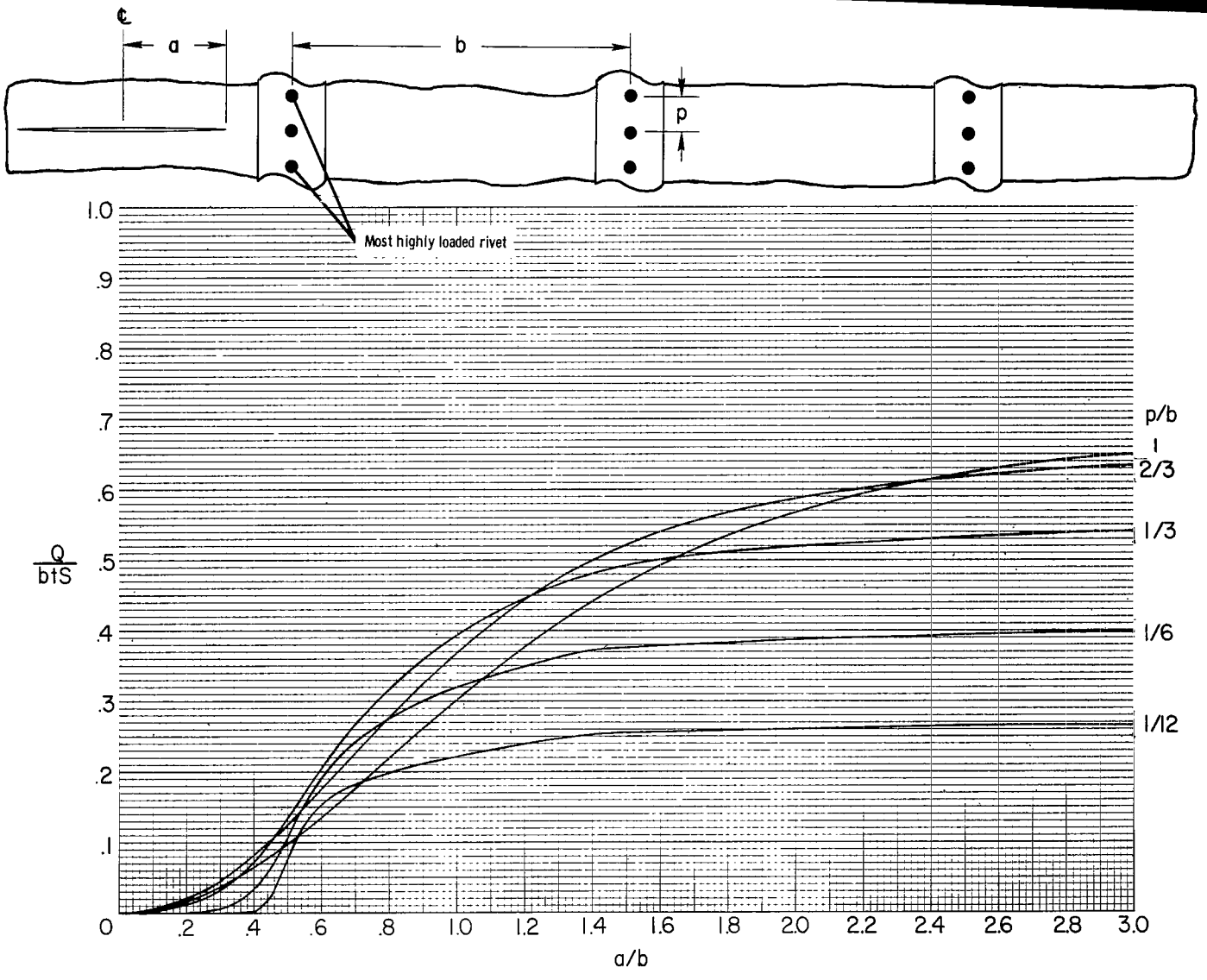

(d) $\mu = 0.50$.

Figure 16.- Continued.

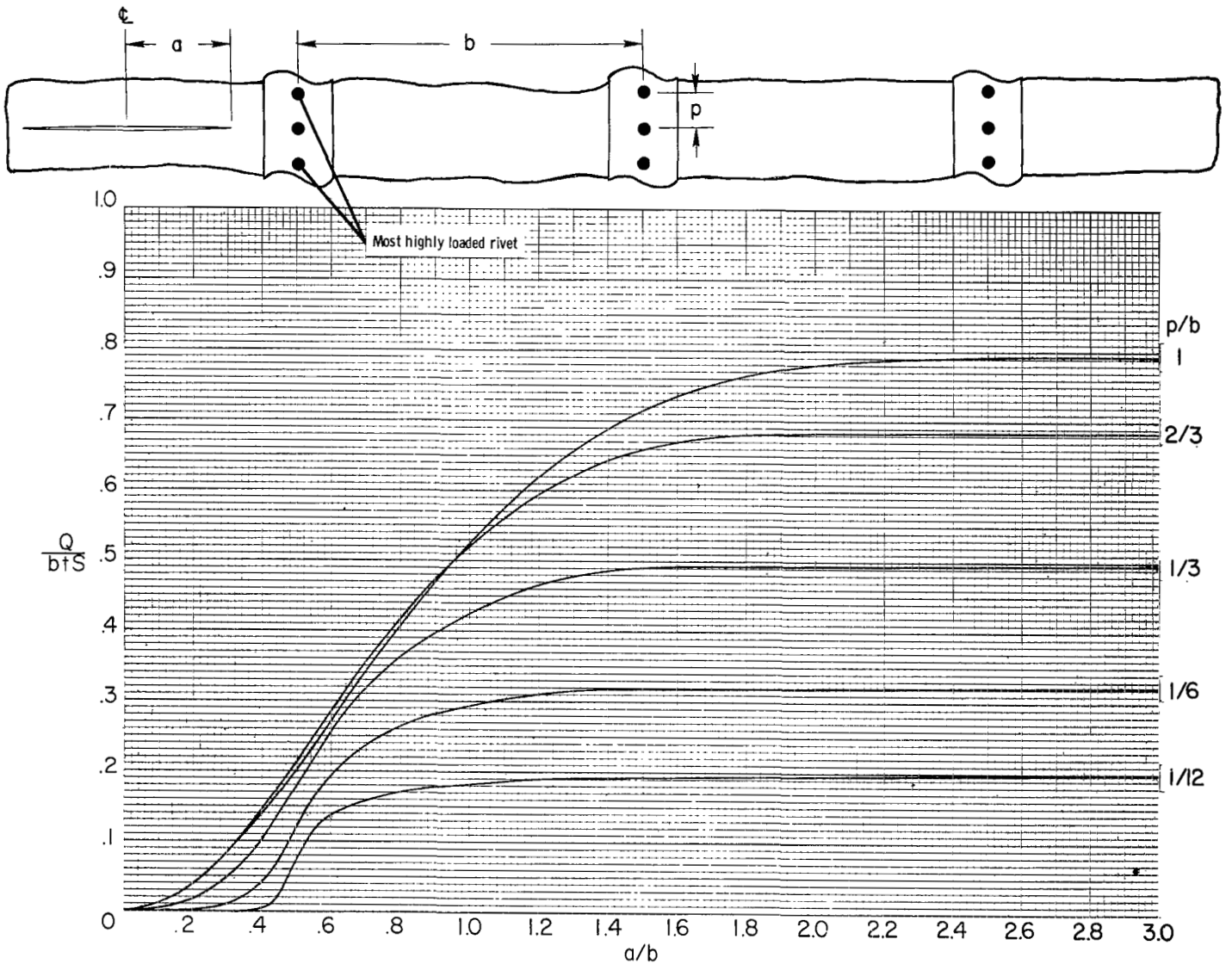

(e) $\mu = 1.00$.

Figure 16.- Concluded.